

QC  
807.5  
U66  
no. 313



# NOAA Technical Report ERL 313-WMPO 5

**U.S. DEPARTMENT OF COMMERCE**  
NATIONAL OCEANIC AND ATMOSPHERIC ADMINISTRATION  
Environmental Research Laboratories

## Spatial and Temporal Variations of the Turbulent Fluxes of Heat, Momentum, and Water Vapor Over Lake Ontario During IFYGL

B.R. BEAN  
C.B. EMMANUEL  
R.O. GILMER  
R.E. McGAVIN

BOULDER, COLO.  
FEBRUARY 1975





## ENVIRONMENTAL RESEARCH LABORATORIES

The mission of the Environmental Research Laboratories is to study the oceans, inland waters, the lower and upper atmosphere, the space environment, and the earth, in search of the understanding needed to provide more useful services in improving man's prospects for survival as influenced by the physical environment. Laboratories contributing to these studies are:

*Atlantic Oceanographic and Meteorological Laboratories (AOML):* Geology and geophysics of ocean basins and borders, oceanic processes, sea-air interactions and remote sensing of ocean processes and characteristics (Miami, Florida).

*Pacific Marine Environmental Laboratory (PMEL):* Environmental processes with emphasis on monitoring and predicting the effects of man's activities on estuarine, coastal, and near-shore marine processes (Seattle, Washington).

*Great Lakes Environmental Research Laboratory (GLERL):* Physical, chemical, and biological limnology, lake-air interactions, lake hydrology, lake level forecasting, and lake ice studies (Ann Arbor, Michigan).

*Atmospheric Physics and Chemistry Laboratory (APCL):* Processes of cloud and precipitation physics; chemical composition and nucleating substances in the lower atmosphere; and laboratory and field experiments toward developing feasible methods of weather modification.

*Air Resources Laboratories (ARL):* Diffusion, transport, and dissipation of atmospheric contaminants; development of methods for prediction and control of atmospheric pollution; geophysical monitoring for climatic change (Silver Spring, Maryland).

*Geophysical Fluid Dynamics Laboratory (GFDL):* Dynamics and physics of geophysical fluid systems; development of a theoretical basis, through mathematical modeling and computer simulation, for the behavior and properties of the atmosphere and the oceans (Princeton, New Jersey).

*National Severe Storms Laboratory (NSSL):* Tornadoes, squall lines, thunderstorms, and other severe local convective phenomena directed toward improved methods of prediction and detection (Norman, Oklahoma).

*Space Environment Laboratory (SEL):* Solar-terrestrial physics, service and technique development in the areas of environmental monitoring and forecasting.

*Aeronomy Laboratory (AL):* Theoretical, laboratory, rocket, and satellite studies of the physical and chemical processes controlling the ionosphere and exosphere of the earth and other planets, and of the dynamics of their interactions with high-altitude meteorology.

*Wave Propagation Laboratory (WPL):* Development of new methods for remote sensing of the geophysical environment with special emphasis on optical, microwave and acoustic sensing systems.

*Marine EcoSystem Analysis Program Office (MPO):* Plans and directs interdisciplinary analyses of the physical, chemical, geological, and biological characteristics of selected coastal regions to assess the potential effects of ocean dumping, municipal and industrial waste discharges, oil pollution, or other activity which may have environmental impact.

*Weather Modification Program Office (WMPO):* Plans and directs ERL weather modification research activities in precipitation enhancement and severe storms mitigation and operates ERL's research aircraft.

NATIONAL OCEANIC AND ATMOSPHERIC ADMINISTRATION

BOULDER, COLORADO 80302





U.S. DEPARTMENT OF COMMERCE

Frederick B. Dent, Secretary

NATIONAL OCEANIC AND ATMOSPHERIC ADMINISTRATION

Robert M. White, Administrator

ENVIRONMENTAL RESEARCH LABORATORIES

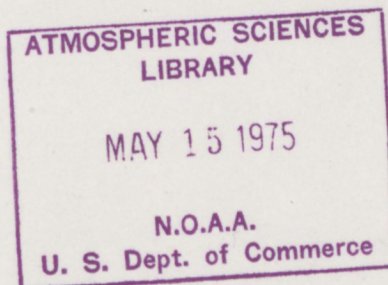
Wilmot N. Hess, Director

QC  
807.5  
-466  
70.313

## NOAA TECHNICAL REPORT ERL 313-WMPO 5

# Spatial and Temporal Variations of the Turbulent Fluxes of Heat, Momentum, and Water Vapor Over Lake Ontario During IFYGL

B.R. BEAN  
C.G. EMMANUEL  
R.O. GILMER  
R.E. McGAVIN



BOULDER, COLO.

February 1975

For sale by the Superintendent of Documents, U. S. Government Printing Office, Washington, D. C. 20402

75 1303







## CONTENTS

	<u>Page</u>
ABSTRACT	1
1. INTRODUCTION	1
2. THE MEASUREMENT OF THE FLUXES OF WATER VAPOR, HEAT, AND MOMENTUM VIA THE EDDY CORRELATION TECHNIQUE	3
3. MEASUREMENTS AND DATA REDUCTION	9
3.1 Measurements	11
3.2 Analysis	11
4. CONCLUSIONS	27
5. REFERENCES	29
APPENDIX A	31
APPENDIX B	40



# SPATIAL AND TEMPORAL VARIATIONS OF THE TURBULENT FLUXES OF HEAT, MOMENTUM, AND WATER VAPOR OVER LAKE ONTARIO DURING IFYGL

B. R. Bean, C. B. Emmanuel, R. O. Gilmer, and R. E. McGavin

During the 1972 IFYGL "alert" periods, the highly instrumented NOAA/RFF/DC-6 aircraft was used to record the time series of wind, temperature, and water vapor at heights ranging from 18 to 300 m above the surface of Lake Ontario. The aircraft was equipped with a gust probe system, a fast response thermistor, a microwave refractometer (for water vapor measurements), and a downward-pointing IR system; as well as the normal in-flight measurement of standard meteorological parameters.

The time series records have been found to display a highly intermittent nature. This is especially the case for evaporation when, in the fall, Polar Continental outbreaks move across the lake. In particular, such an outbreak of cold dry air moved across the lake at  $12\text{--}15\text{ m s}^{-1}$  on 9 October 1972. This resulted in the air temperature at 30 m above the lake to drop from 12 to 6 C while the evaporation rate increased to more than  $1\text{ cm day}^{-1}$ . This may be compared with the  $0.5\text{ cm day}^{-1}$  normal evaporation observed in the tropics during BOMEX. Furthermore, IR lake surface temperatures show cold regions ( $\sim 5\text{ C}$ ) along the north shore, presumably due to strong upwelling, while the center and south shore regions of the lake were of the order of 12 to 15 C. The turbulent flux quantities of momentum, heat, and water vapor were obtained by the eddy correlation technique and their spectra were determined at several locations over the lake surface for 3-minute sampling lengths. At the aircraft speed of  $92\text{ m s}^{-1}$ , this represents a flight path of  $\sim 17\text{ km}$  for both along wind and constant fetch patterns. The spectra demonstrate the tendency for the peak value to march to higher wavelengths with increasing height.

## 1. INTRODUCTION

Heretofore the process of evaporation from large bodies of water has been studied by various techniques, including the water budget, energy balance, and bulk-aerodynamic methods (Webb, 1960). The water budget method is heavily dependent upon metering water flow into and out



of the lake or reservoir, and the quantities measured require long-term averages. The result is that they yield evaporation estimates for periods of about a week. The bulk-aerodynamic method must rely on the assumption of an empirical relationship between the wind and humidity profiles over the water surface. Frenkiel (1963) concluded that for the combined energy budget and bulk-aerodynamic methods there is no firm basis for regarding any evaporation fluctuations less than 20 percent as falling outside the range of random experimental errors, even under the most favorable assumptions.

Measurement of evaporation over short periods would be very desirable, for then the diurnal cycle of evaporation could be ascertained. The eddy correlation technique (Swinbank, 1951; Bean et al., 1969) shows great promise. In this formulation, the eddy flux of water vapor is expressed as

$$E = \overline{\rho_w' w'} \quad [\text{g m}^{-2}\text{s}^{-1}], \quad (1)$$

where  $E$  is the evaporation,  $\rho_w$  is the water vapor density, and  $w$  is the vertical component of the wind velocity. The primes denote departures of these quantities from their respective mean values. The overbar denotes a time average, normally of the order of a few minutes, rather than the many hours or days required by other techniques. The details of this technique as well as its accuracy are discussed in subsequent sections of this report.

Because of the nature of the physical environment, the measurement of evaporation via the eddy correlation technique, as well as the fluxes of heat and momentum, over a large body of water has been extremely difficult to accomplish. In recent years, however, properly instrumented aircraft have contributed much to our capability of making such measurements and subsequently increased our knowledge of the marine boundary layer (Bean et al., 1972; Grossman and Bean, 1973; McBean and Paterson, 1974). This has become possible because of the availability of precise, fast-response wind gust sensors, as well as sensors that sample the temperature and water vapor fields from mesoscale horizontal distances to scales of a few tens of meters within short periods of time: 3 to 10 minutes.

An adequate description of the planetary boundary layer over a limited fetch body of water requires measurements of the spatial and temporal variations of the fluxes of water vapor, heat, and momentum. In this report we present the work of the Boundary Layer Dynamics Group, Office of Weather Modification, ERL/NOAA, on the direct measurement of these fluxes over Lake Ontario. The work was performed during the joint U.S.-Canadian cooperative studies at Lake Ontario, commonly referred to as the International Field Year for the Great Lakes (IFYGL). The extensive measurements, taken during the IFYGL "alert" periods in 1972, from land-based sensors, buoys, and aircraft should prove most useful in parameterization techniques necessary for the understanding of the physical processes involved in the interaction of the air-water fields at Lake Ontario.



## 2. THE MEASUREMENT OF THE FLUXES OF WATER VAPOR, HEAT, AND MOMENTUM VIA THE EDDY CORRELATION TECHNIQUE

The eddy correlation technique defines the flux value of a particular quantity as

$$F_x = x w , \quad (2)$$

where  $w$  represents the vertical component of the wind and  $x$  denotes the quantity whose flux value we are attempting to determine. Evaporation from a water surface is defined as the amount of water vapor carried aloft from unit area per unit time; hence,

$$E = \rho_w w , \quad (3)$$

where  $\rho_w$  is the water vapor density ( $\text{g m}^{-3}$ ), and  $w$  is the vertical component of the wind ( $\text{m s}^{-1}$ ). Normally the determination of evaporation implies a time average of both  $\rho_w$  and  $w$ . Consequently, if we express the instantaneous values of  $\rho_w$  and  $w$  as being composed of a mean value (denoted by an overbar) and a fluctuating (about the mean value) quantity (denoted by a prime), then

$$\begin{aligned} \rho_w &= \overline{\rho_w} + \rho_w' \\ w &= \overline{w} + w' \end{aligned} \quad (4)$$

Substituting (4) into (3) and averaging, we obtain

$$E = (\overline{\rho_w} + \overline{\rho_w'}) (\overline{w} + \overline{w'}) . \quad (5)$$

Upon expanding (5) and invoking the Reynolds rules of averaging, we obtain

$$E = \overline{\rho_w' w'} + \overline{\rho_w} \overline{w} , \quad (6)$$

where the first term on the right is the eddy flux. For sufficiently long averaging times,  $\overline{w} \equiv 0$ , hence

$$E = \overline{\rho_w' w'} \quad [\text{g m}^{-2}\text{s}^{-1}] , \quad (7)$$

which states that the eddy flux of water vapor is equal to the evaporation. The averaging time which is inherent in this formulation is important. Swinbank (1955) found that the minimum sample size to insure



the presence of all the flux information of a passive parameter was of the order of 100 seconds. If the sample is too long, the diurnal cycle will affect the results and thus destroy stationarity. Any sample size in excess of 100 seconds but less than 1 hour, except at sunrise and sunset, should provide an adequate averaging interval.

Expression (7) represents actually the covariance between the water vapor and the vertical wind. This implies that some correlation exists between the two variables whenever evaporation occurs, and as such it should be noted when the effect of errors in the determination of evaporation is considered.

The covariance between two variables, say  $X$  and  $Y$ , is defined as

$$\text{Cov}(X,Y) \equiv \overline{(X-\bar{X})(Y-\bar{Y})} . \quad (8)$$

Now let us assume that a constant bias is present in each of the measurements, such that

$$X = X_T + \epsilon$$

$$Y = Y_T + \delta$$

where the subscript  $T$  represents the true values while  $\epsilon$  and  $\delta$  are the biases of measurement. Substitution in (8) yields

$$\text{Cov}(X,Y) = \overline{[X_T + \epsilon - (\bar{X}_T + \epsilon)][Y_T + \delta - (\bar{Y}_T + \delta)]} . \quad (9)$$

Since  $\epsilon$  and  $\delta$  are constant, (9) becomes

$$\text{Cov}(X,Y) = (X_T - \bar{X}_T)(Y_T - \bar{Y}_T) , \quad (10)$$

indicating that a constant bias in either measurement has no effect on the accuracy of the measurement.

If, however, we assume that  $\epsilon$  and  $\delta$  are normally distributed random errors then, upon expansion, (9) yields

$$\text{Cov}(X,Y) = \text{Cov}(X_T, Y_T) + \text{Cov}(\epsilon, Y_T) + \text{Cov}(\delta, Y_T) + \text{Cov}(\epsilon, \delta) . \quad (11)$$

The last three terms of this expression represent the effects of the error in measurement. If the measurement of  $X$  is independent of the measurement of  $Y$ , and, therefore, the error in measuring  $X$  is not related



to the error in measuring  $Y$ , then these terms are essentially zero since they are the covariances between independent variables. This does not imply that  $X$  and  $Y$  are independent but merely that the error in the measurement of  $X$  is independent of the error in the measurement of  $Y$ .

An entirely similar approach is used in determining of the heat and momentum fluxes. In summary, we have

- i) Water vapor flux  $\equiv \overline{\rho_w' w'}$   $[g\ m^{-2}s^{-1}]$ ,
- ii) Heat (Temp) flux  $\equiv \overline{T' w'}$   $[m\ K\ s^{-1}]$ ,
- iii) Momentum flux  $\equiv \overline{u' w'}$   $[m^2s^{-1}]$ .

The platform used for all the measurements during IFYGL was the instrumented NOAA/RFF/DC-6 aircraft, figure 1. The aircraft, among other instrumentation, was equipped with a gust probe system, a fast response thermistor, a microwave refractometer (fig. 1), and a downward pointing IR system. The wind field measurements were made via the two vanes that are near the tip of the boom. Strain gauges are fixed to the vanes and record the force exerted by the air motion. These forces are then related to angular deflections of the vanes (in this manner, the fixed vanes measure an angle of attack relative to the airstream). The details of the gust probe system are given in Appendix A. In addition, at the very tip of the boom there is a pitot tube which records air motion as small pressure fluctuations. The remaining instrumentation on the boom consists of a fast response thermistor for recording the air temperature fluctuations and a microwave cavity for the measurement of the short-term fluctuations of the radio refractive index. The latter are then translated into short-term fluctuations of the water vapor density.

The microwave refractometer, originally designed by Birnbaum (1950), has undergone many changes in recent years to improve its operation and stability. The fundamental principle of the instrument is based on the relationship between the resonant frequency  $f$  of a microwave cavity, its dimensions  $K$ , and the refractive index,  $n$ , of the contents, i.e.,

$$f = - Kn, \quad (12)$$

or

$$\frac{\Delta f}{f} = - \frac{\Delta n}{n} \approx - \Delta n, \quad (13)$$

since  $n \approx 1.000300$ . Thus, the relative change in the refractive index of the air inside a microwave cavity is equal to the relative change in the resonant frequency (if the operating frequency is 10 GHz and if the change in the refractive index is 1 part per million (ppm), then the resonant frequency of the cavity will change by 10 kHz).



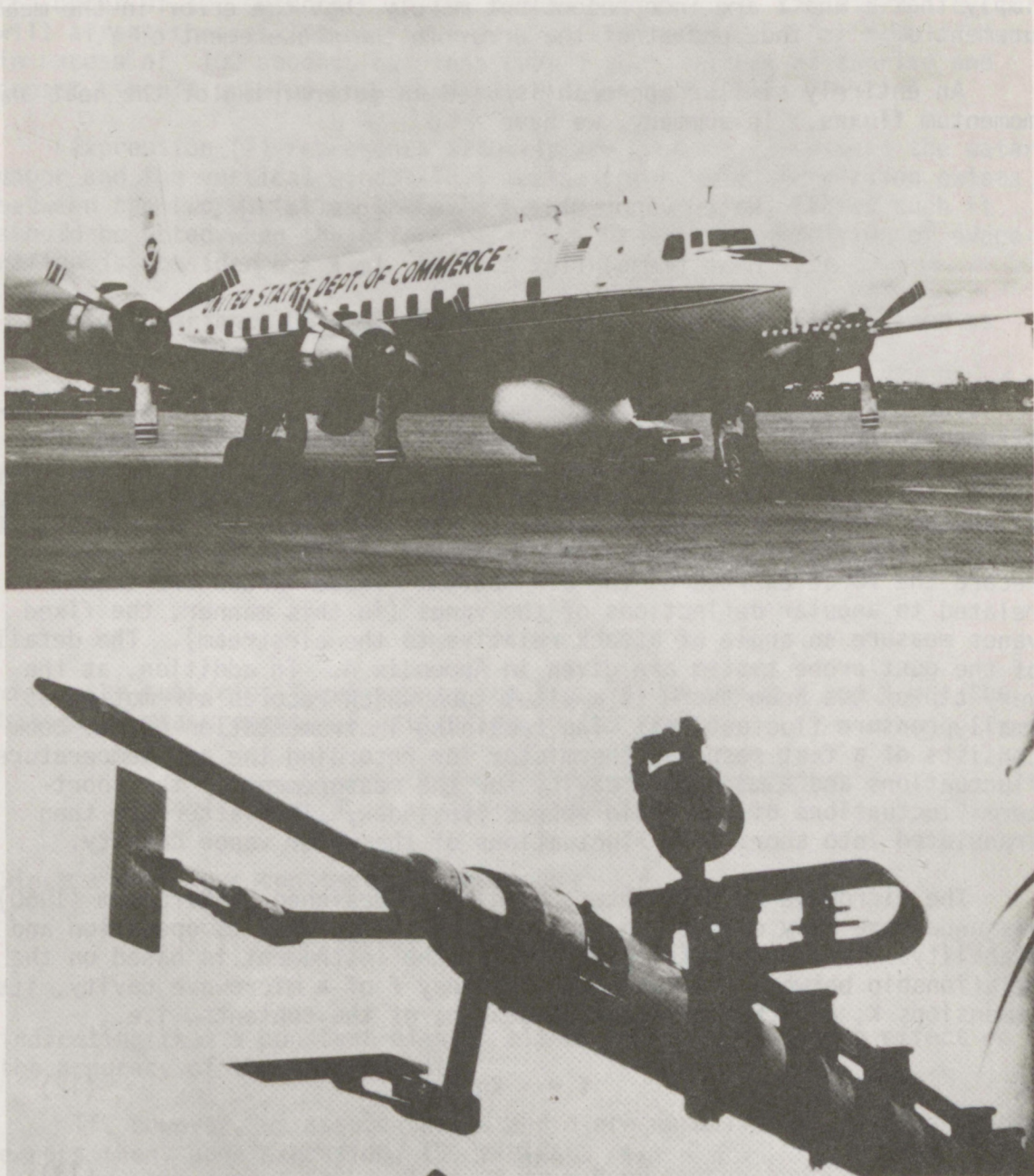


Figure 1. (Top): The NOAA Research Flight Facility (RFF)  
DC-6 research aircraft.  
(Bottom): The quiet probe system.



When a sealed cavity is used as a reference, then the difference between the resonant frequencies of the sampling cavity and the reference cavity represents a measure of the refractive index of the air passing through the sampling cavity. Since the refractive index,  $n$ , is a number such as 1.000300, it has been common practice to scale the index up, i.e.,

$$N = (n-1) \times 10^6, \quad (14)$$

where  $N$  is referred to as the refractivity and is related to meteorological parameters via

$$N = 77.6 \frac{P}{T} + 1.72 \times 10^3 \frac{\rho_w}{T}. \quad (15)$$

In this expression  $P$  is the total pressure in mb,  $T$  is the temperature in  $^{\circ}\text{K}$ , and  $\rho_w$  is the water vapor density in  $\text{g m}^{-3}$  (Bean and Dutton, 1966). Solving for  $\rho_w$ , (15) yields

$$\rho_w = 5.81 \times 10^{-4} NT - 4.51 \times 10^{-2} P. \quad (16)$$

Accuracies of 1 ppm in refractive index with resolution of one part in  $10^8$  became common. As a result, measurements in the absolute humidity to within  $0.2 \text{ gm}^{-3}$  with a resolution of  $0.02 \text{ g m}^{-3}$  (equivalent to a 2 percent maximum error at standard sea level conditions) were easily achieved (McGavin and Vetter, 1965).

The gust probe defines a coordinate system which, being fixed to the aircraft, has three degrees of freedom with respect to a coordinate system referenced to the earth and translating with the aircraft. These degrees of freedom are known as roll, pitch, and yaw and are rotations about the  $x$ ,  $y$ , and  $z$  axes, respectively, of the earth-referenced coordinate system. The gust probe data, however, cannot be correctly interpreted if they are analyzed with respect to the aircraft coordinate system.

The inertial platform aboard the aircraft represents an earth referenced coordinate system which is independent of the aircraft roll, pitch, and yaw. As a result, the inertial platform is able to accurately determine the roll, pitch, and yaw angles. By use of these angles the gust sensed in the aircraft coordinate system is referenced to the inertial platform coordinate system. This places the gust in a stationary coordinate system where the gusts have some physical meaning.



Grossman and Bean (1973) have performed a detailed error analysis for the airborne gust probe system used during BOMEX. The same system was used during the Lake Ontario measurements. Here we summarize the pertinent findings of their work on the error analysis. In all, the measurements of 16 parameters are needed for the determination of the fluxes of heat, momentum, and water vapor. Since the data are detrended, the absolute accuracy of each measurement is of little concern; the error is a function of the resolution of the various instruments. Table 1 summarizes the pertinent results; these are the root-sum-square (rss) errors contributed by the independent sensors. Table 1 also gives the expected errors in the individual values and the error in the mean over each complete sample.

Table 1. Errors (rss) due to Response of Sensors of the Airborne Gust Probe System

Parameter	Units	Error	Typical Range of Values
Errors expected in the individual values			
$u'$	$\text{m s}^{-1}$	$2 \times 10^{-2}$	1.0
$w'$	$\text{m s}^{-1}$	$6 \times 10^{-2}$	0.3
$T'$	$^{\circ}\text{K}$	$0.5 \times 10^{-2}$	0.4
$\rho_w'$	$\text{g m}^{-3}$	$1 \times 10^{-2}$	0.6
$u'w'$	$\text{m}^2 \text{s}^{-2}$	$1.2 \times 10^{-2}$	4.0
$T'w'$	$^{\circ}\text{K m s}^{-1}$	$1.2 \times 10^{-2}$	0.4
$\rho_w'w'$	$\text{g m}^{-2} \text{s}^{-1}$	$1.2 \times 10^{-1}$	4.0
Error expected in the mean			
$\overline{u'w'}$	$\text{m}^2 \text{s}^{-2}$	$7 \times 10^{-6}$	$10^{-1}$
$\overline{T'w'}$	$^{\circ}\text{K m s}^{-1}$	$12 \times 10^{-5}$	$8 \times 10^{-4}$
$\overline{\rho_w'w'}$	$\text{g m}^{-2} \text{s}^{-1}$	$2.7 \times 10^{-6}$	$6 \times 10^{-2}$



### 3. MEASUREMENTS AND DATA REDUCTION

Figure 2 shows a map of the Lake Ontario basin and the locations (shaded area) where measurements were taken during the IFYGL "alert" periods. Appendix B gives the dates/times as well as the levels of measurements.

The reduction of the gust probe measurements to velocities is achieved via the expression

$$V_{\ell} = T \cdot U_m + (\hat{i} \cdot \vec{\alpha}_{\ell}) dt + \hat{i} \cdot (\vec{\Omega} \times \vec{T} \cdot L) \quad (17)$$

where the definitions of all terms are given in table 2. In this expression the first term on the right represents the gusts in the aircraft

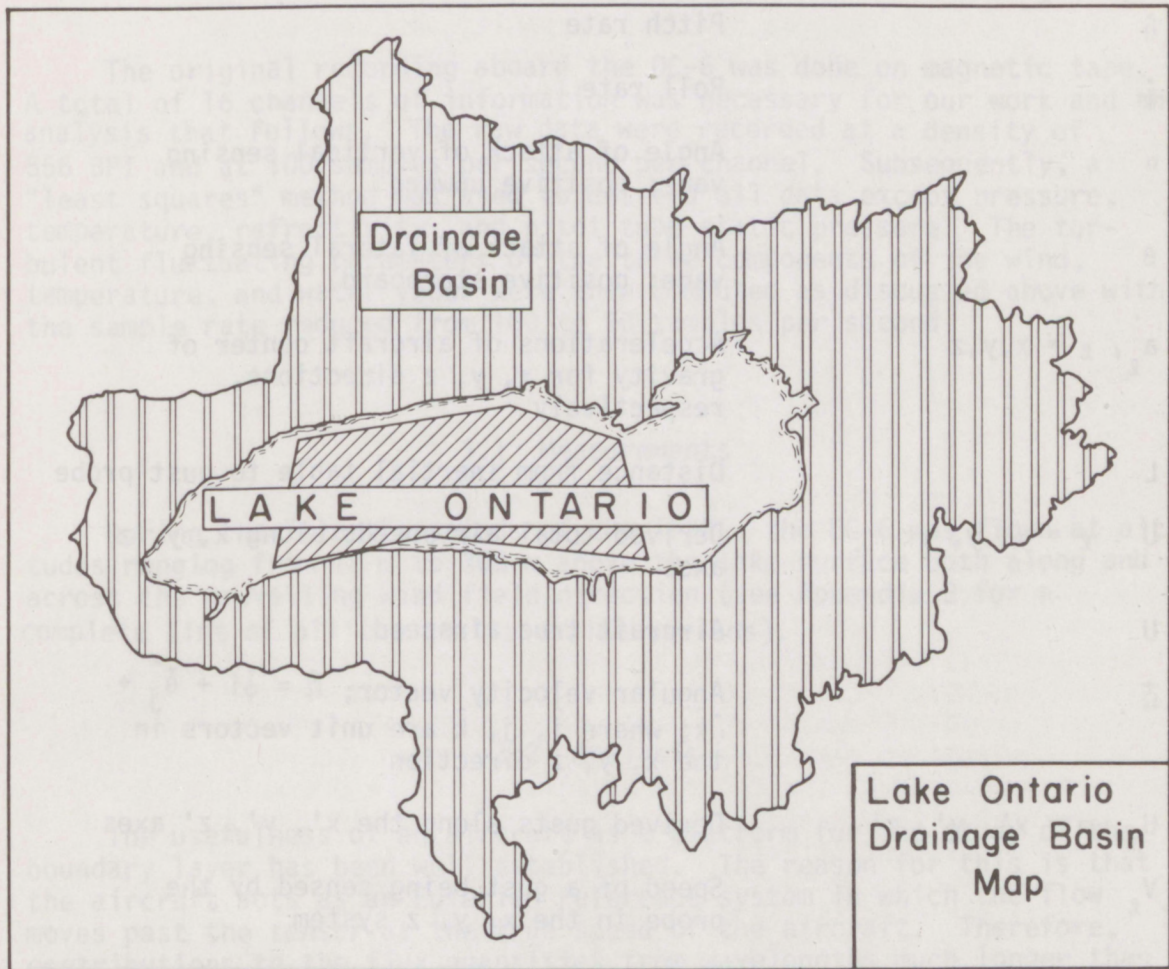


Figure 2. Lake Ontario with shaded area showing regions of intensive measurements during IFYGL.



Table 2. Notation used in Derivation of Gust Equation

Symbol	Definition
$\psi$	Yaw angle; a rotation about the aircraft vertical axis; positive with nose of aircraft to starboard
$\theta$	Pitch angle; a rotation about the aircraft longitudinal axis; positive nose upward
$\phi$	Roll angle; a rotation about the aircraft longitudinal axis; positive right wing down
$\dot{\psi}$	Yaw rate
$\dot{\theta}$	Pitch rate
$\dot{\phi}$	Roll rate
$\alpha$	Angle of attack of vertical sensing vane; positive upward
$\beta$	Angle of attack of lateral sensing vane; positive starboard
$a_{\ell}, \ell = x, y, z$	Accelerations of aircraft center of gravity for x, y, z directions, respectively
L	Distance from inertial table to gust probe
$U_{\ell}, \ell = x, y, z$	Derived total air speeds along x, y, z axes
U	Aircraft true airspeed
$\vec{\Omega}$	Angular velocity vector; $\vec{\Omega} = \dot{\phi}\hat{i} + \dot{\theta}\hat{j} + \dot{\psi}\hat{k}$ ; where $\hat{i}, \hat{j}, \hat{k}$ are unit vectors in the x, y, z direction
$U_m, m = x', y', z'$	Derived gusts along the x', y', z' axes
$V_{\ell}$	Speed of a gust being sensed by the probe in the x, y, z system



coordinate system and transformed to the platform coordinate system; the second term represents the calculated translational velocities of the platform coordinate system based upon the inertial platform accelerations relative to the earth, and finally the third term represents a correction to account for the rotation of the aircraft coordinate system relative to the platform coordinate system. For a more detailed description of the gust equations the reader is referred to Bean et al. (1972). When all the necessary transformations are performed, the final equations for the horizontal and vertical wind fluctuations become

$$\begin{aligned} u' &= U \cos(\alpha-\theta) - L \sin\theta - [\bar{U} \cos(\bar{\alpha}-\bar{\theta}) - L \sin\bar{\theta}] \\ w' &= U \sin(\alpha-\theta) + \alpha_z dt + L \cos\theta - [\bar{U} \sin(\bar{\alpha}-\bar{\theta}) + \bar{\alpha}_z dt \\ &\quad + L \cos\bar{\theta}] . \quad (18) \end{aligned}$$

The original recording aboard the DC-6 was done on magnetic tape. A total of 16 channels of information was necessary for our work and the analysis that follows. The raw data were recorded at a density of 556 BPI and at 100 samples per second per channel. Subsequently, a "least squares" method was used to detrend all data except pressure, temperature, refractivity, and pitot tube static pressure. The turbulent fluctuating parameters of the three components of the wind, temperature, and water vapor were then computed as discussed above with the sample rate reduced from 100 to 50 samples per second.

### 3.1 Measurements

During the "alert" periods of the IFYGL, the DC-6 was flown at altitudes ranging from 18 m to 300 m above the lake surface both along and across the prevailing wind field direction (see Appendix B for a complete list of all the analyzed time periods).

### 3.2 Analysis

The usefulness of an aircraft as a platform for the study of the boundary layer has been well established. The reason for this is that the aircraft acts as an Eulerian reference system in which the flow moves past the sensor at the true speed of the aircraft. Therefore, contributions to the flux quantities from wavelengths much longer than those normally measured from fixed platforms are accounted for. The horizontal resolution of the gust probe system as used during the IFYGL was from 8.4 m (the low pass filter cut-off) to 8.4 km (half the flight path length equivalent to a 3-minute run).



From the original data tapes the calibrated and detrended time series records were constructed at 50 samples per second. From these records, 3-minute time segments were chosen for analysis; mean values of the three components of the wind ( $u$ ,  $v$ ,  $w$ ), temperature ( $T$ ), and water vapor density ( $\rho_w$ ) as well as their flux quantities were determined.

The resulting time series of  $u'$ ,  $w'$ ,  $T'$ ,  $\rho_w'$  and those of the flux quantities were spectrum analyzed by means of a fast Fourier transform technique. For convenience in the interpretation of the data, the spectral as well as the cospectral densities were multiplied by frequency so that in the case of the cospectra, the area under the curve is proportional to the energy when plotted with linear ordinate [ $fP(f)$ ] and log abscissa [ $f$ ].

We now discuss in some detail the results obtained on two particular days — 11 May and 9 October 1972. The former represents what is considered to be a "normal" day and the latter represents an "active" day. These classifications are totally arbitrary, at best, and are used here simply as reference days against which the results of other days may be compared. October 9 is unusual because a Polar Continental outbreak moved across the lake and the aircraft was able to make extensive measurements throughout the lake.

Figures 3, 4, and 5 present the time series records for the turbulent fluctuating components of the wind ( $u'$ ,  $v'$ ,  $w'$ ); the water vapor density ( $\rho_w$ ), and the temperature ( $T$ ). Figure 3 gives the turbulent parameters flying 3-minute legs at constant fetch at several levels above the lake surface. Figure 4 presents the same information but for flight legs parallel to the wind direction at approximately 10 km south of the north shore of the lake (in the vicinity of Cobourg, Canada). As expected, the temperature and water vapor density fluctuations exhibit a high correlation (negative) in all the records. Table 3 summarizes the pertinent statistics for each 3-minute time segment.

In general, this particular day exhibited small negative heat, water vapor and momentum flux; the only exception being those values obtained on the flight path shown on figure 5. This particular flight, however, exhibits a structure reminiscent of that found on measurements taken when breaking waves of the Kelvin-Helmholtz type are present (Woods, 1969; Browning, 1971; Emmanuel, 1972; 1973). Note the general appearance of the turbulent fluctuations in all the quantities. Those pertaining to  $w'$  have an average descending motion of 8.75 s which corresponds to a horizontal scale of  $\sim 814$  m at the aircraft speed of  $92 \text{ m s}^{-1}$ . The ascending portion takes place in  $\sim 14.3$  s which corresponds to  $\sim 1330$  m. At the same time,  $\rho_w'$  and  $T'$  exhibit high (negative) correlation. Also, a slight lag is found between the minima in  $T'$  and  $u'$ . Furthermore, the broad maximum values of  $\rho_w'$  and minimum values of  $T'$  and  $u'$  compared with the saw-tooth structure of  $w'$  suggest the aircraft was traversing a



Table 3. Statistics for Each 3-minute Time Segment on 11 May 1972

Level [m]	$\overline{u'w'}$ [ $\text{m}^2\text{s}^{-2}$ ]	$\overline{w'T'}$ [ $\text{m}^2 \text{K s}^{-1}$ ]	$\overline{\rho_w'w'}$ [ $\text{cm day}^{-1}$ ]
30	-0.100	0.009	0.002
90	0.078	0.024	-0.021
150	-0.000	-0.011	0.037
300	-0.121	-0.016	-0.033
18	-0.047	-0.023	0.035
30	0.496	0.099	0.048
90	-0.077	-0.034	0.103
150	-0.389	-0.007	-0.004
30	-0.034	-0.016	-0.030
150	-0.821	1.013	-1.272

region of breaking waves. In addition, during this time the aircraft experienced three to four "bumps." The surface temperature of the lake during this entire flight did not exhibit any large variations; the surface temperature did not vary by more than 0.1C, so that we may exclude the possibility of thermal plumes. The surface temperature of the lake was much less than the air temperature at 30 m. In fact, strong, positive temperature gradients persisted during the day over the entire lake. On the average, the surface temperature was approximately 2C while the temperature at 30 m was in the neighborhood of 10C and at 90 m it was 14C. The temperature was nearly constant between 90 and 300 m.

October 9 was the first day in the IFYGL "evaporation year" that a cold Polar Continental outbreak moved over the lake. During the day the winds were steady over the entire lake blowing out of the northwest at about  $12 \text{ m s}^{-1}$  at an altitude of 30 m. The continuous and strong winds had a pronounced effect on both the surface temperature distribution of the lake and the temperature at 30 m. Figure 6 gives the surface temperature distribution obtained on two flight paths from Cobourg to Sodus Bay and back to Cobourg. Bathymetric maps indicate that there is a sharp increase in the depth of the lake approximately 10 km south-south-east of Cobourg. The induced wind drag on the lake surface due to the persistently strong winds resulted in considerable upwelling currents from the north shore to about 5-10 km off-shore. The surface temperature distribution is shown in figure 7. Figure 8 shows the white convergence zone separating the cold and warm masses of water as observed on the following day, October 10. Also shown in the figure is the surface IR temperature trace as the aircraft crossed the white "streak."

As in the case for the May data, the original time series records were used to extract the time series of the turbulent fluctuating



11 May 1972

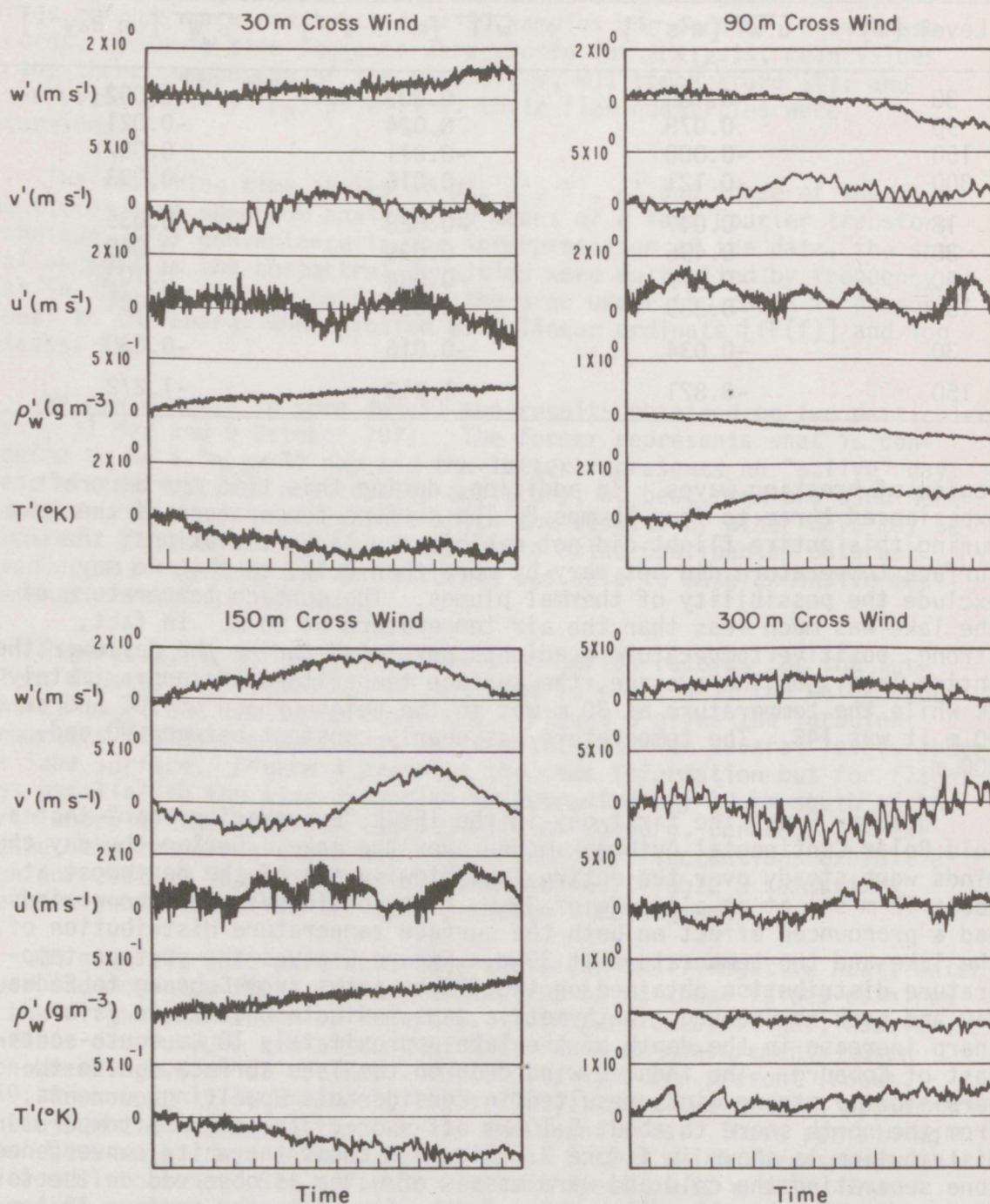


Figure 3. Time series records for the fluctuating components of the wind ( $u'$ ,  $v'$ ,  $w'$ ), the water vapor density ( $\rho'_w$ ), and the temperature ( $T'$ ) for the height levels shown. The abscissa represents time with each "tick" mark equivalent to 10 s. The flight path was normal to the wind direction.



11 May 1972

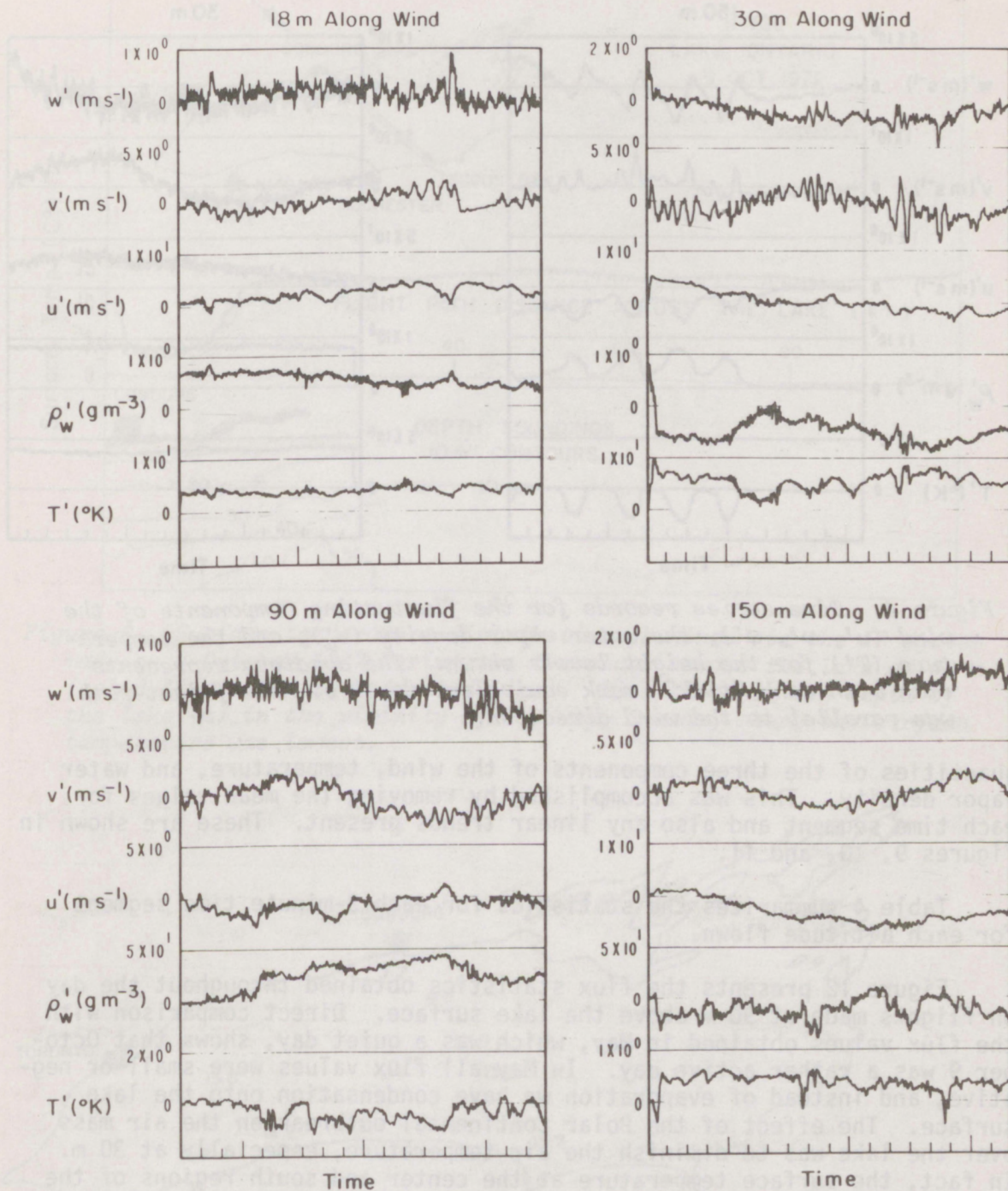


Figure 4. Time series records for the fluctuating components of the wind ( $u'$ ,  $v'$ ,  $w'$ ), the water vapor density ( $\rho'_w$ ), and the temperature ( $T'$ ) for the height levels shown. The abscissa represents time with each "tick" mark equivalent to 10 s. The flight path was parallel to the wind direction.



11 May 1972

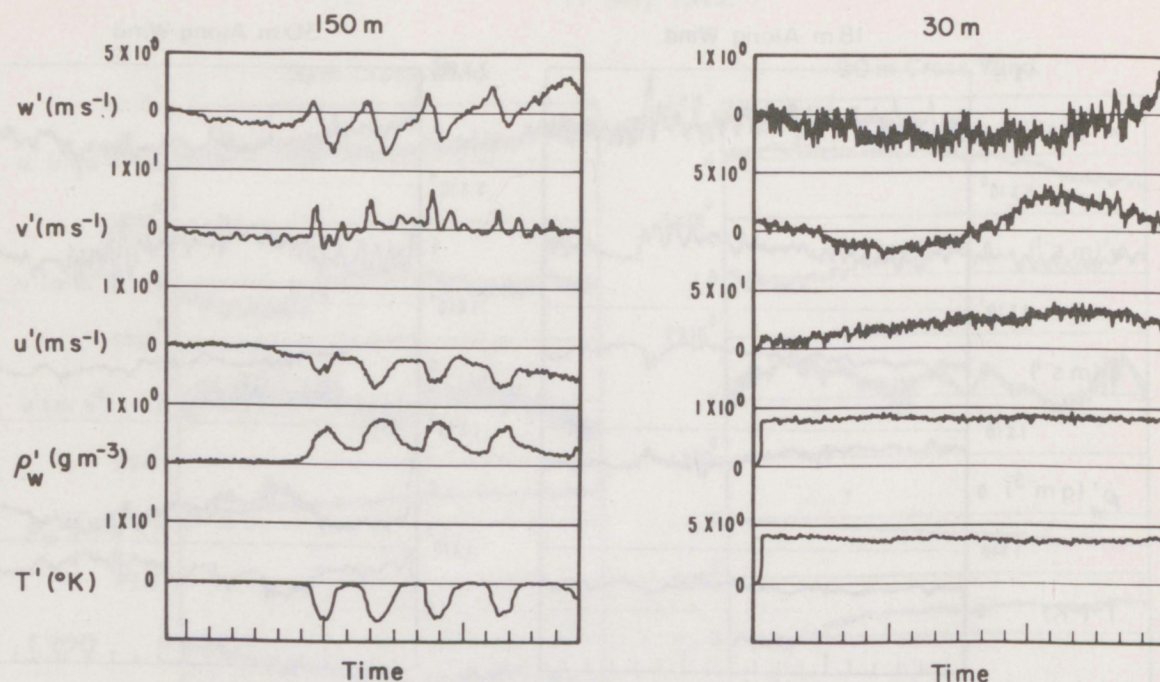


Figure 4. Time series records for the fluctuating components of the wind ( $u'$ ,  $v'$ ,  $w'$ ), the water vapor density ( $\rho'_w$ ), and the temperature ( $T'$ ) for the height levels shown. The abscissa represents time with each "tick" mark equivalent to 10 s. The flight path was parallel to the wind direction.

quantities of the three components of the wind, temperature, and water vapor density. This was accomplished by removing the mean values for each time segment and also any linear trends present. These are shown in figures 9, 10, and 11.

Table 4 summarizes the statistics for each 3-minute time segment for each altitude flown.

Figure 12 presents the flux statistics obtained throughout the day on flights made at 90 m above the lake surface. Direct comparison with the flux values obtained in May, which was a quiet day, shows that October 9 was a rather active day. In May all flux values were small or negative, and instead of evaporation we have condensation onto the lake surface. The effect of the Polar Continental outbreak on the air mass over the lake was to diminish the air temperature, especially at 30 m. In fact, the surface temperature at the center and south regions of the lake was nearly twice that at the 30 and 90 m levels. A marked increase in evaporation is evident from north to south of the lake normal to the prevailing wind field, perhaps due to building surf and resultant spray from white caps. Independent measurements (McBean and Paterson, 1974) of the turbulent fluxes made on the same day, although not necessarily at the same location, height, and time agree well with those reported



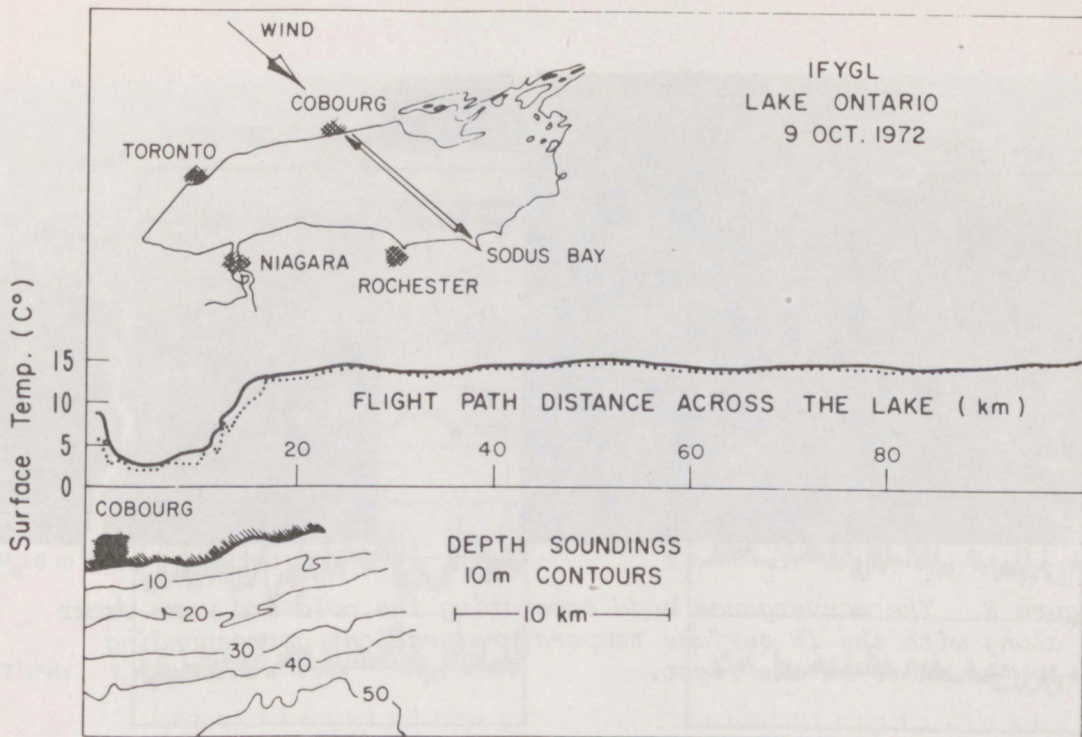


Figure 6. Surface temperature distribution obtained via the IR system made on 9 October 1972 during two traverses across the lake at 90 m (solid line) and 150 m (dotted line). Also shown is the depth of the lake (m) in the vicinity of Cobourg, Canada, where the surface temperature was lowest.

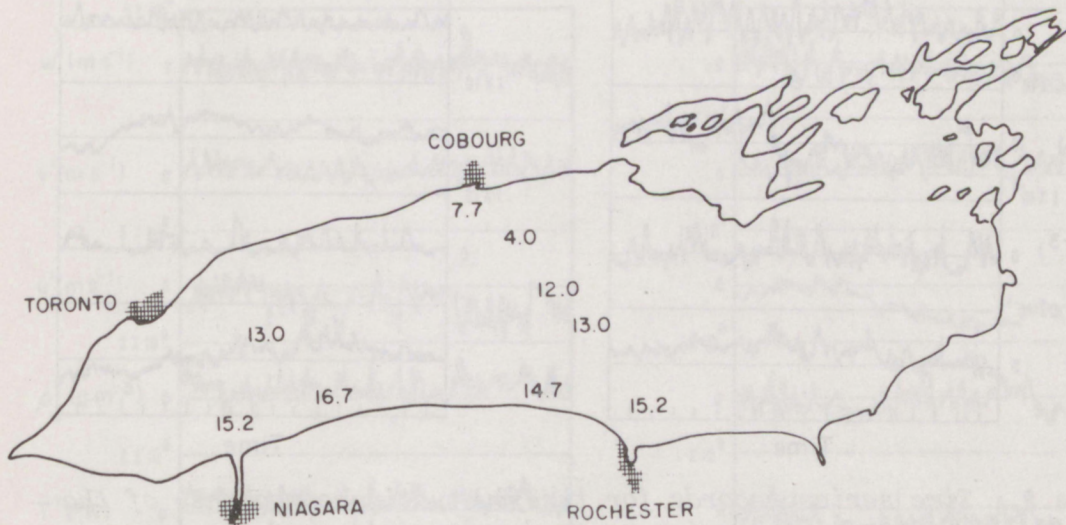


Figure 7. The surface temperature distribution (°C) obtained on 9 Oct 1972



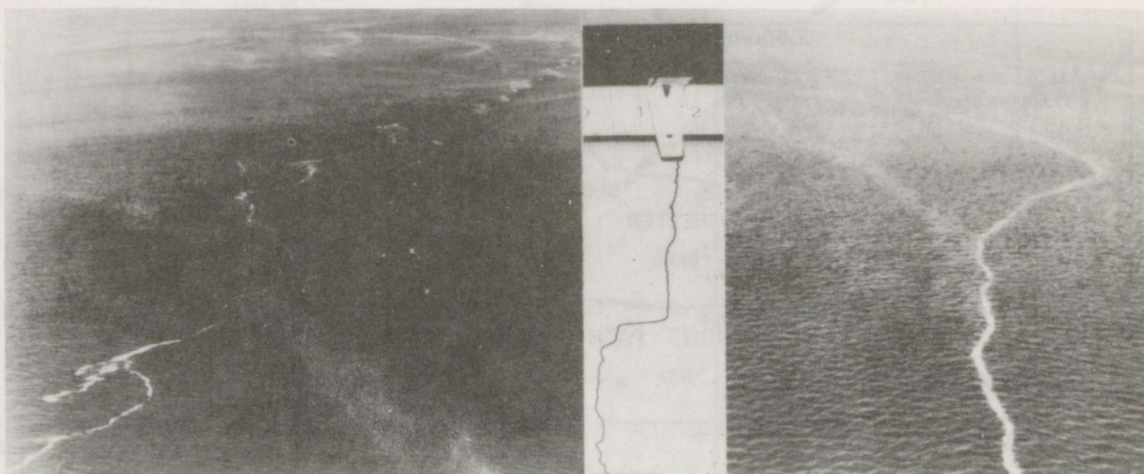


Figure 8. The convergence zone separating the cold and warm water along with the IR surface temperature gradient corresponding to the photo on the right.

9 October 1972

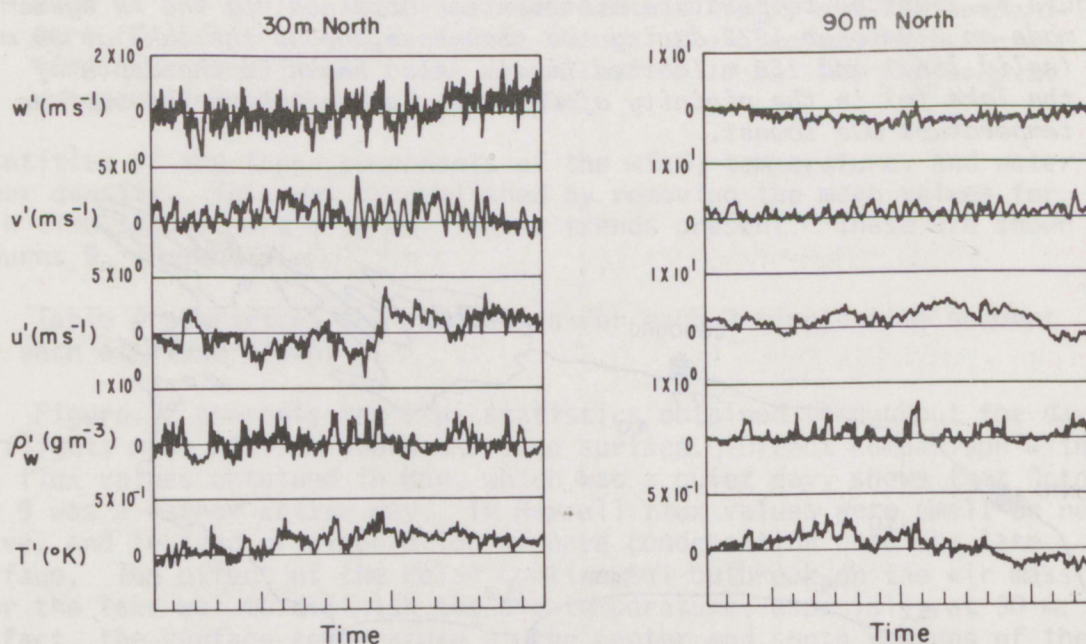


Figure 9. Time series records for the fluctuating components of the wind ( $u'$ ,  $v'$ ,  $w'$ ), the water vapor density ( $\rho'_w$ ), and the temperature ( $T$ ) for the height levels shown. The abscissa represents time with "tick" mark equivalent to 10 s. The flight was normal to the wind obtained on 9 October 1972 near the northern shore of the lake.



9 October 1972

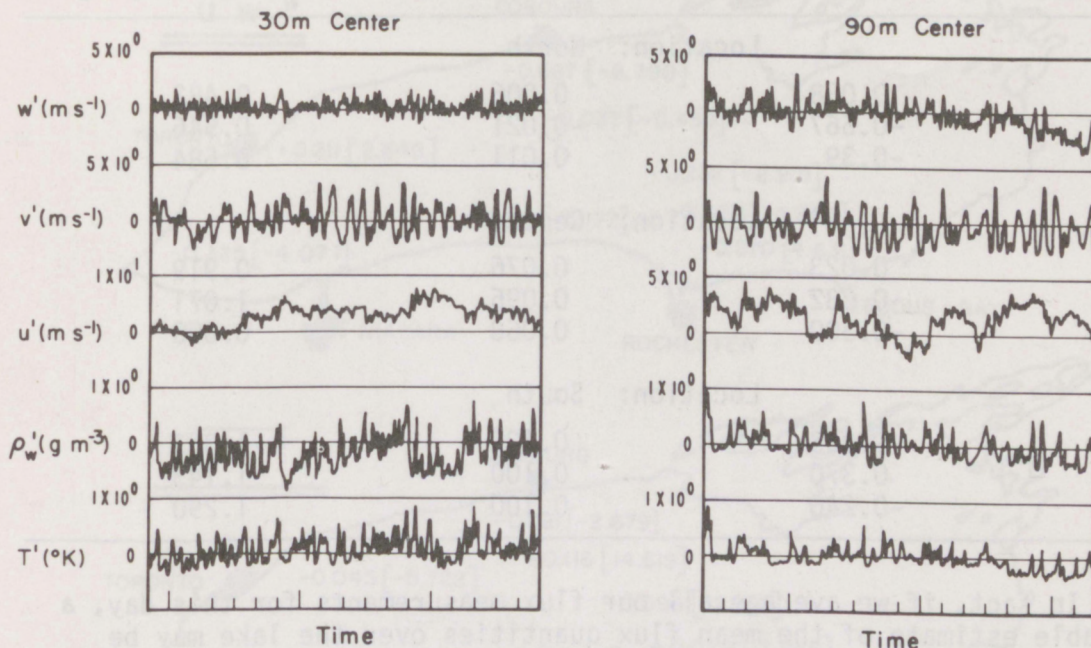


Figure 10. Same as Fig. 9. The flight path was normal to the wind obtained on 9 Oct 1972 near the center of the lake.

9 October 1972

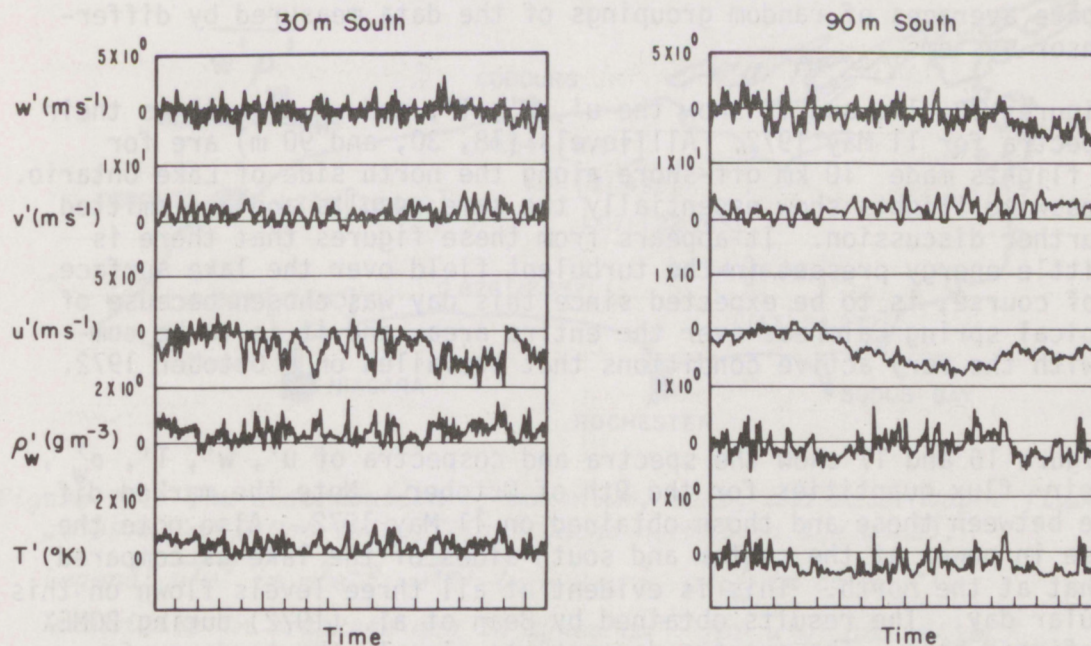


Figure 11. Same as Fig. 9. The flight path was normal to the wind obtained on 9 Oct 1972 near the south shore of the lake.



Table 4. Statistics of the Fluxes for 9 October 1972

Level [m]	$\overline{u'w'}$ [ $\text{m}^2\text{s}^{-2}$ ]	$\overline{w'T'}$ [ $\text{m K s}^{-1}$ ]	$\overline{\rho'_w w'}$ [ $\text{cm day}^{-1}$ ]
Location: North			
30	0.088	0.006	0.482
90	-0.667	-0.021	0.546
150	-0.39	0.011	0.584
Location: Center			
30	0.023	0.076	0.919
90	-0.232	0.096	1.071
150	-0.300	0.060	0.600
Location: South			
30	-0.363	0.120	1.363
90	0.370	0.100	1.143
150	-0.240	0.100	1.290

here. In fact, if we average all our flux measurements for this day, a reasonable estimate of the mean flux quantities over the lake may be made. The values we obtain at the 90 m level for momentum, heat, and evaporation are  $0.18 \text{ m}^2 \text{ s}^{-2}$ ,  $6.3 \text{ mW cm}^{-2}$ , and  $21.8 \text{ mW cm}^{-2}$ , respectively. The results of McBean and Paterson for the 150 m level are found to be  $0.14 \text{ m}^2 \text{ s}^{-2}$ ,  $4.4 \text{ mW cm}^{-2}$ , and  $24.7 \text{ mW cm}^{-2}$ , respectively. Indeed, this kind of agreement appears to be as good as we would expect if we were to compare averages of random groupings of the data measured by different sensor systems.

Figures 13, 14, and 15 show the  $u'$ ,  $w'$ ,  $T'$ , and  $\rho'_w$  as well as their flux spectra for 11 May 1972. All levels (18, 30, and 90 m) are for upwind flights made 10 km off-shore along the north side of Lake Ontario. The crosswind flights show essentially the same results and are omitted from further discussion. It appears from these figures that there is very little energy present in the turbulent field over the lake surface. This, of course, is to be expected since this day was chosen because of its typical spring calmness over the entire area, and it is to be compared with the very active conditions that prevailed on 9 October 1972.

Figure 16 and 17 show the spectra and cospectra of  $u'$ ,  $w'$ ,  $T'$ ,  $\rho'_w$ , and their flux quantities for the 9th of October. Note the marked difference between these and those obtained on 11 May 1972. Also note the increase in power at the center and south sides of the lake as compared with that at the north. This is evident at all three levels flown on this particular day. The results obtained by Bean et al. (1972) during BOMEX are confirmed here. The spectra demonstrate clearly the tendency for



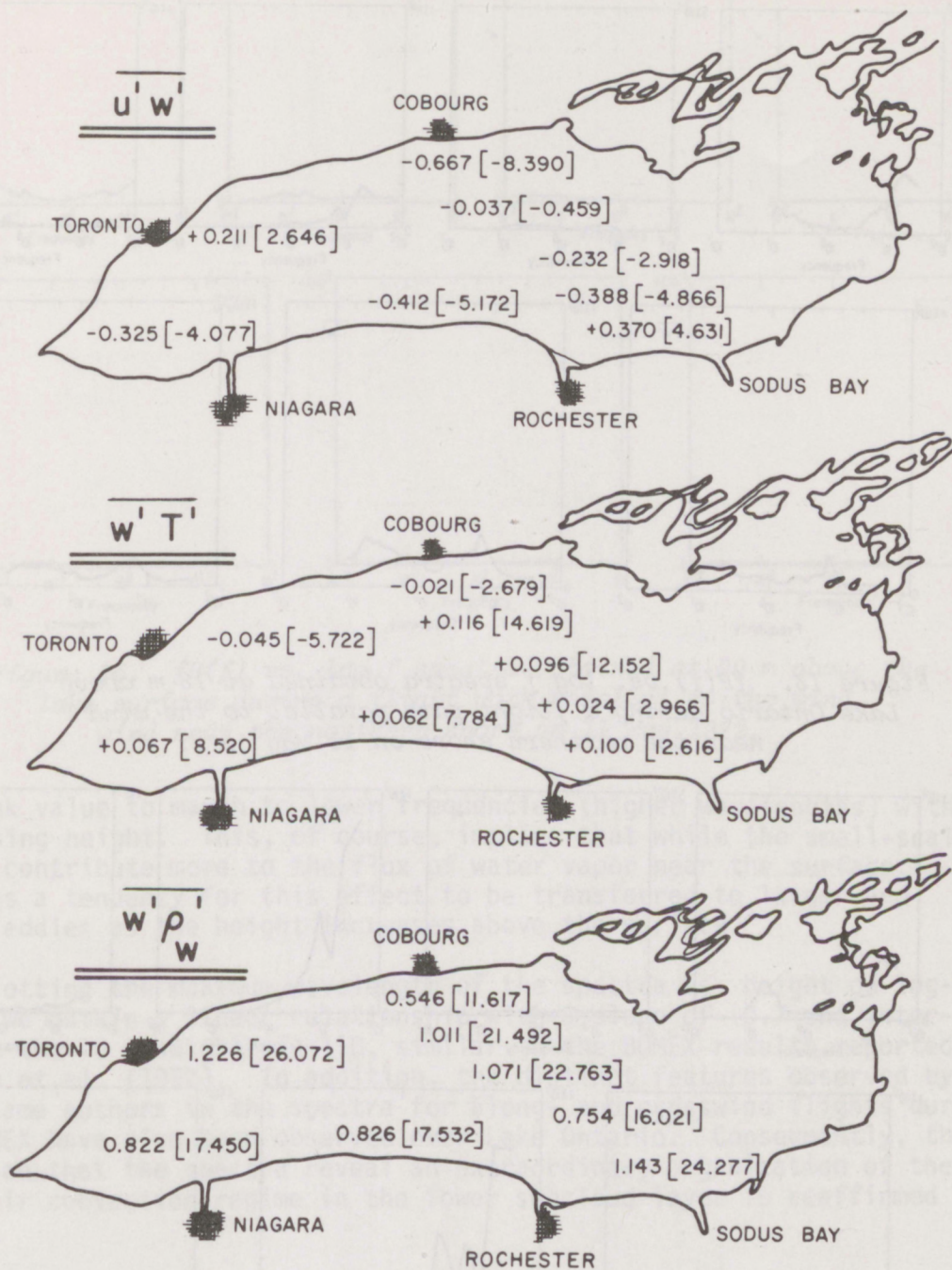


Figure 12. The distribution of momentum, heat, and water vapor fluxes at 90 m for 9 Oct 1972 (flight paths normal to the wind).

Legend:  $\overline{u'w'}$  in m<sup>2</sup>s<sup>-2</sup>,  $\overline{w'T'}$  in m K s<sup>-1</sup>,  $\overline{w'\rho_w'}$  in cm day<sup>-1</sup>.

Quantities in brackets are in dynes cm<sup>-2</sup> for  $\overline{u'w'}$  and mW cm<sup>-2</sup> for  $\overline{w'T'}$  and  $\overline{w'\rho_w'}$ .



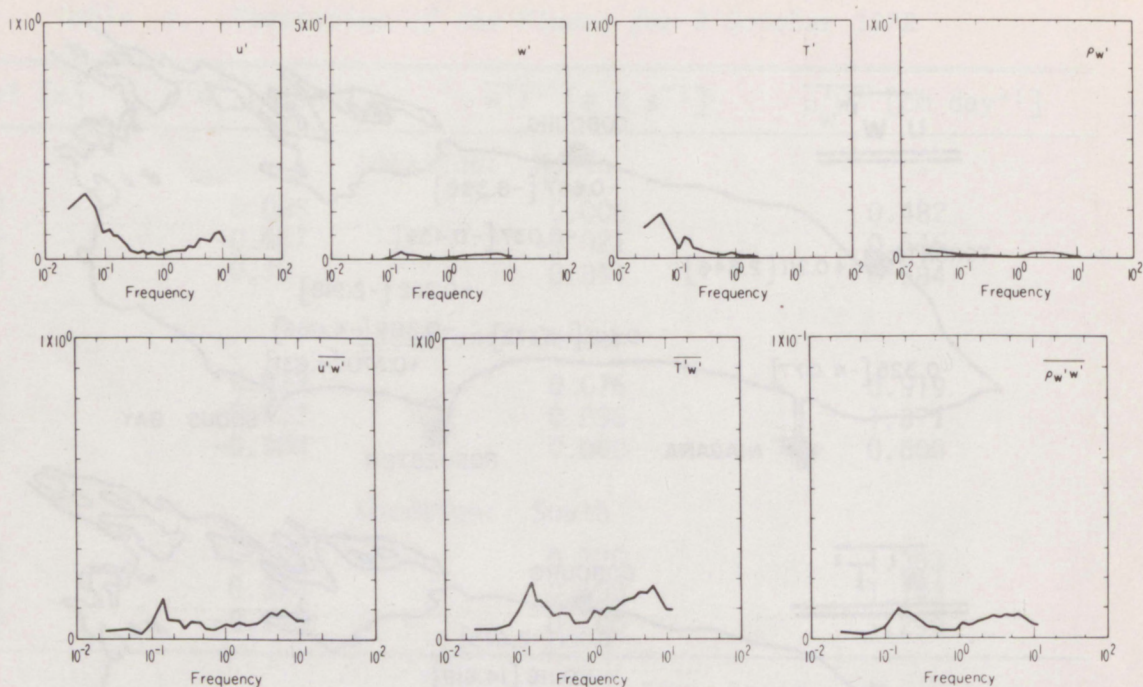


Figure 13.  $fP(f)$  vs.  $\log f$  spectra obtained at 18 m above Lake Ontario during a flight path parallel to the wind near the northern shore on 11 May 1972.

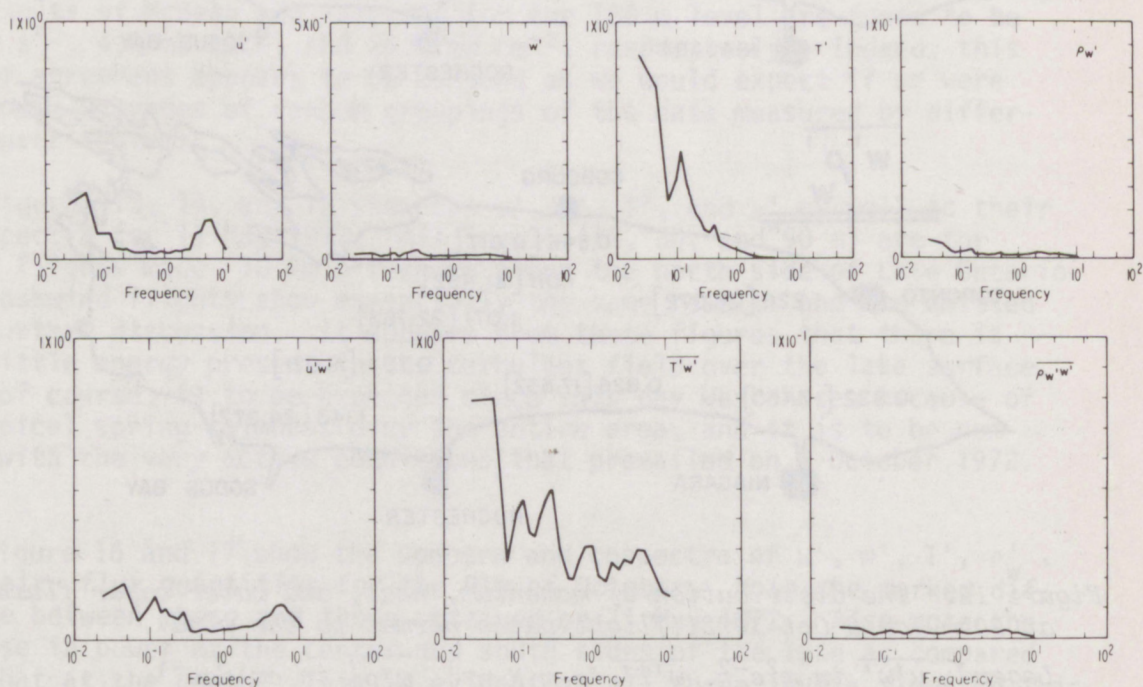


Figure 14.  $fP(f)$  vs.  $\log f$  spectra obtained at 30 m above the lake surface during a flight path parallel to the wind near the northern shore on 11 May 1972.



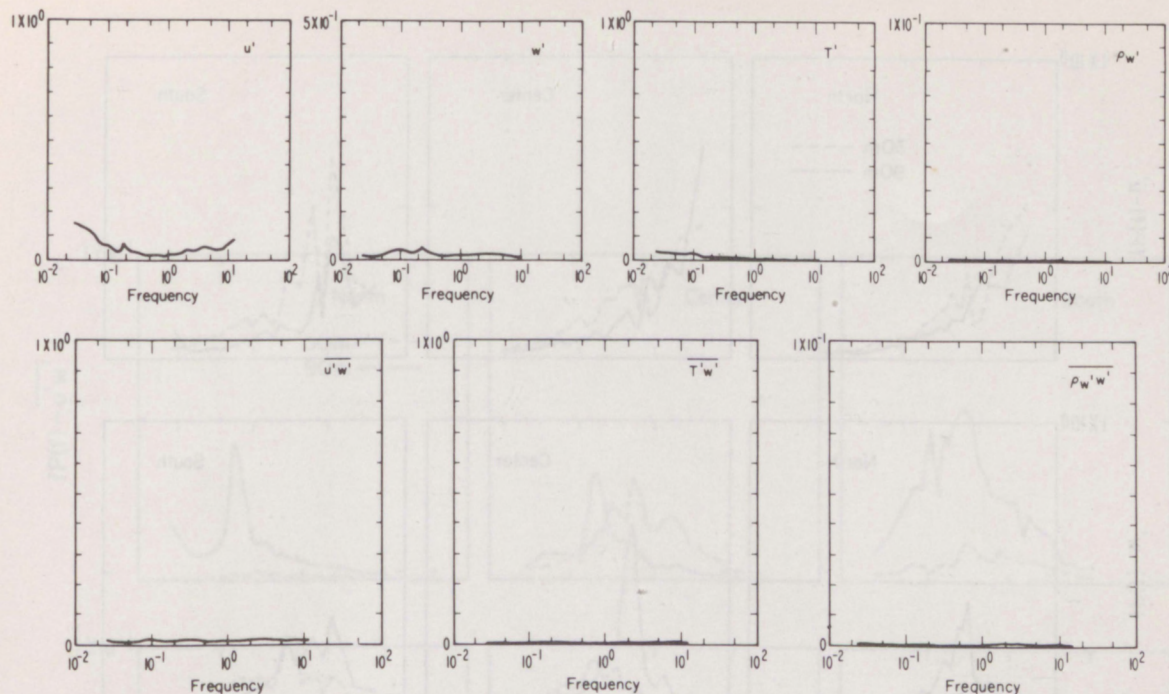


Figure 15.  $fP(f)$  vs.  $\log f$  spectra obtained at 90 m above the lake surface during a flight path parallel to the wind near the northern shore on 11 May 1972.

the peak value to march to lower frequencies (higher wavelengths) with increasing height. This, of course, implies that while the small-scale eddies contribute more to the flux of water vapor near the surface, there is a tendency for this effect to be transferred to larger and larger eddies as the height increases above the surface.

Plotting the maximum wavelength of the spectra vs. height on log-log paper, we obtain a linear relationship with a slope of  $\sim 0.7$  and intercept at the 10 m height of 110, similar to the BOMEX results reported by Bean et al. (1972). In addition, the distinct features observed by these same authors in the spectra for along- and crosswind flights during BOMEX have also been observed over Lake Ontario. Consequently, their assertion that the spectra reveal an extraordinary organization of the clear air convection regime in the lower subcloud layer is reaffirmed here.

Figure 18 shows the  $P(f)$  spectra of momentum, heat, and water vapor density at 30 m level for the north, center, and south areas of the lake for 9 October 1972.

The results obtained for 10 October 1972 are identical to those presented for the previous day and are not shown here. The magnitudes of the fluxes are slightly lower reflecting the fact that the prevailing winds had diminished slightly, but the overall picture of events remained unaltered.



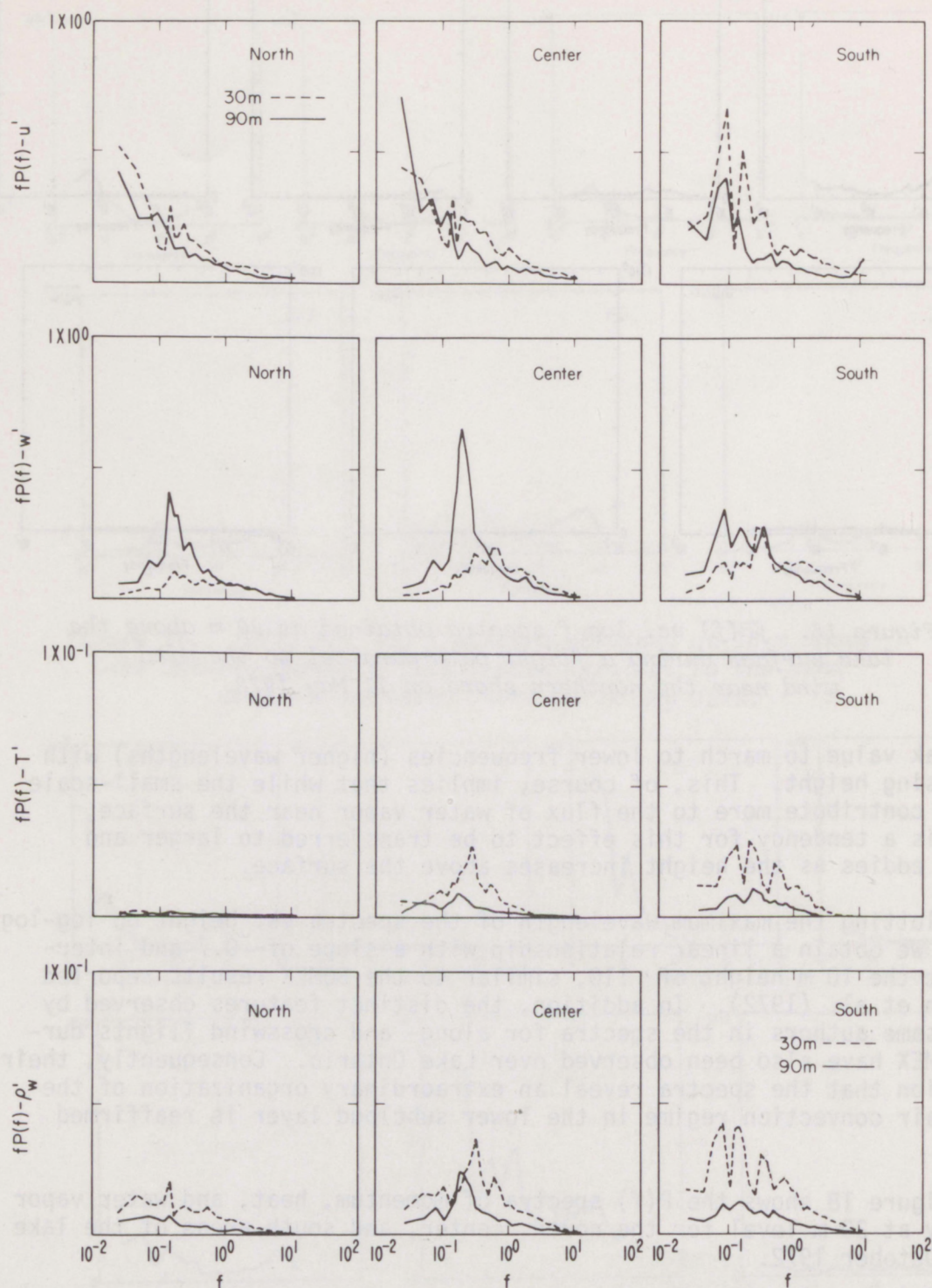


Figure 16. Spectra of  $u'$ ,  $w'$ ,  $T'$ , and  $\rho'_w$  obtained during flights normal to the wind. The dotted line is for flights made at 30 m above the lake surface, the solid for 90 m. All flights were on 9 Oct 1972.



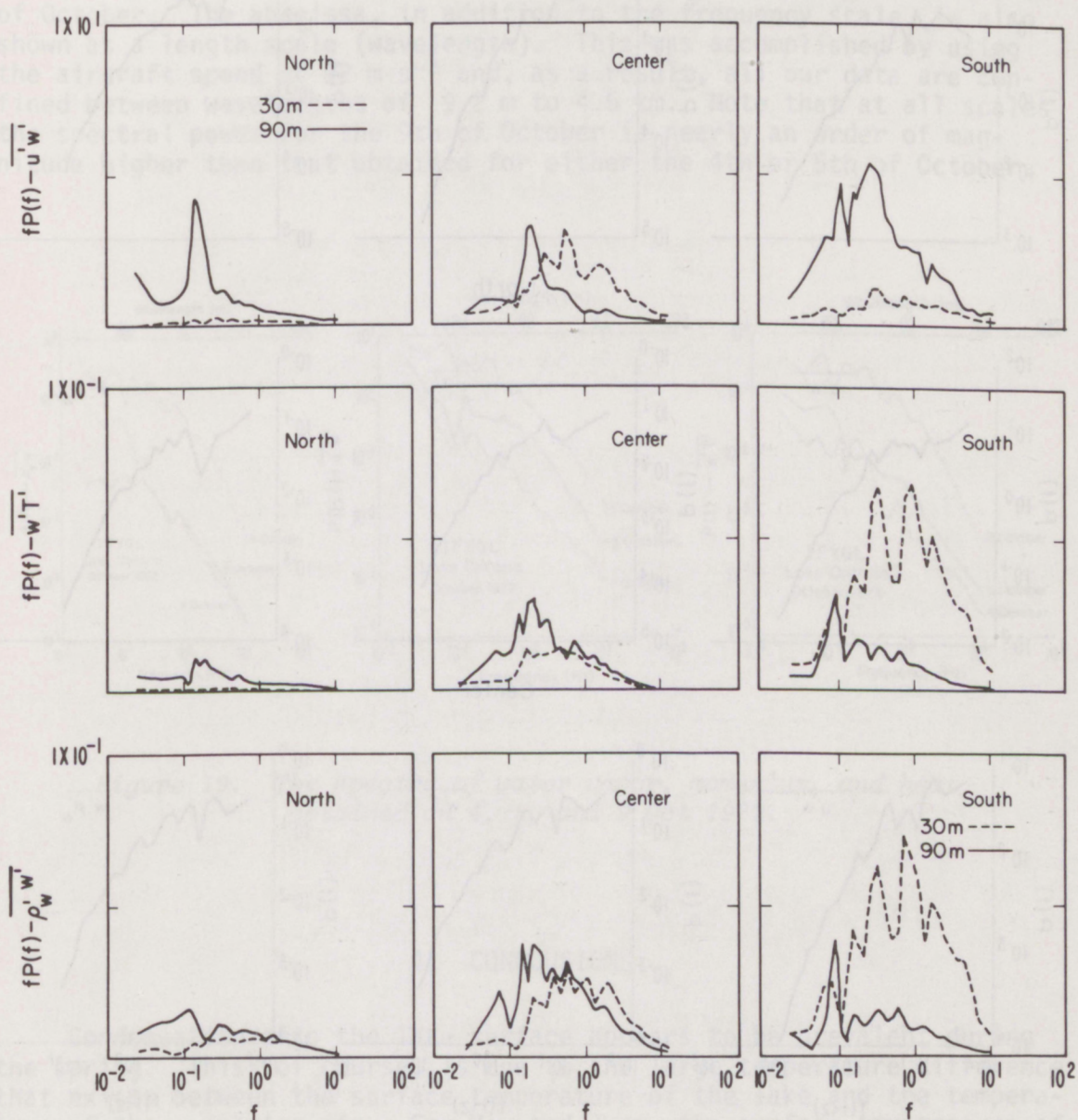


Figure 17. The spectra of the flux quantities obtained during flights normal to the wind. The dotted line is for flights made at 30 m above the lake surface, the solid for 90 m. All flights were on 9 Oct 1972.



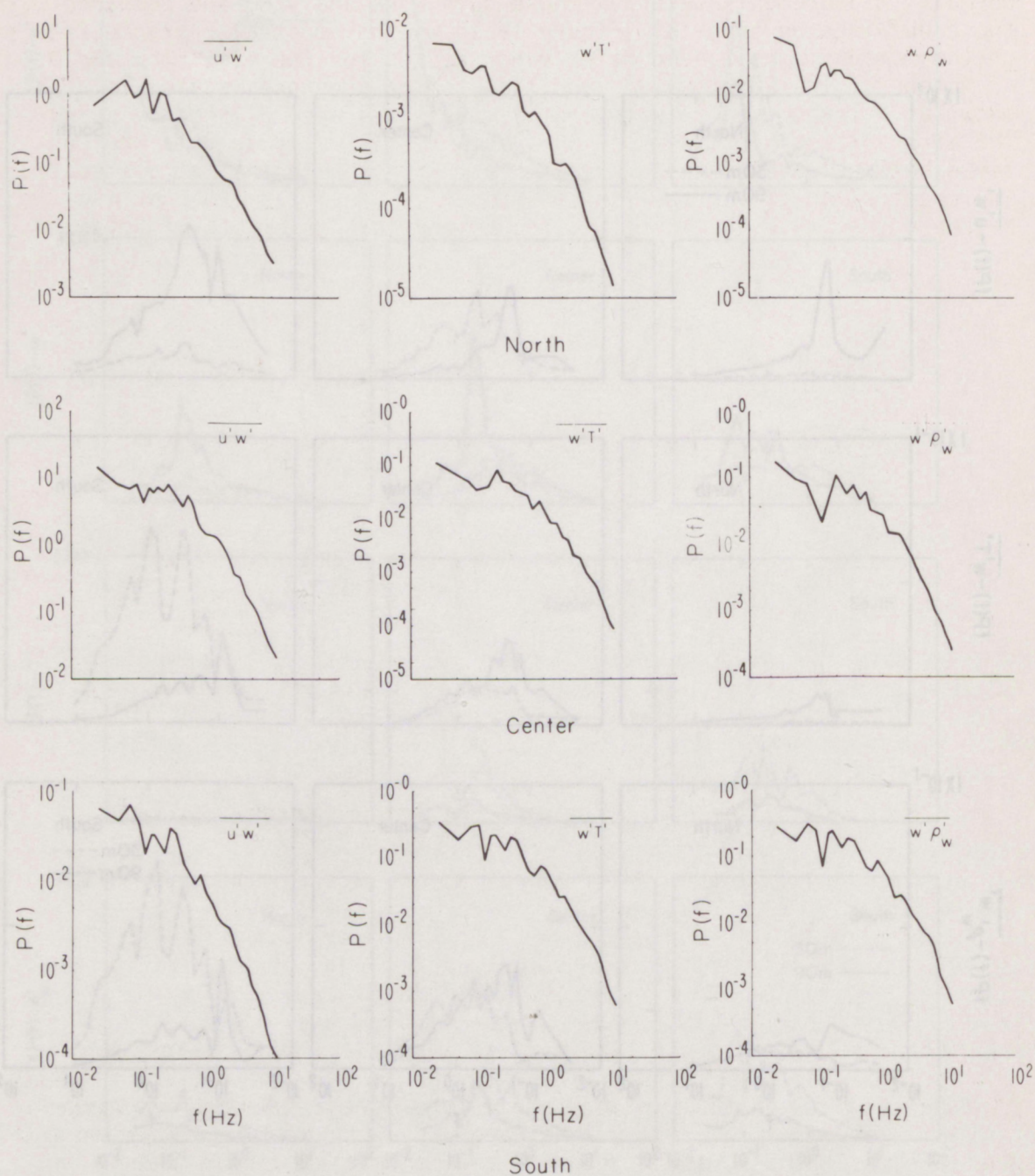


Figure 18. Spectra of momentum, heat, and water vapor,  
9 Oct. 1972



In early October and in particular on the 4th and 5th, the prevalent atmospheric conditions over the Lake Ontario basin were considered to be normal. Measurements taken on those days were analyzed and compared with those obtained on the 9th. Figure 19 shows the spectral characteristics of the momentum, heat, and water vapor fluxes for the 4th, 5th, and 9th of October. The abscissa, in addition to the frequency scale, is also shown as a length scale (wavelength). This was accomplished by using the aircraft speed of  $92 \text{ m s}^{-1}$  and, as a result, all our data are confined between wavelengths of 9.2 m to 4.6 km. Note that at all scales the spectral power for the 9th of October is nearly an order of magnitude higher than that obtained for either the 4th or 5th of October.

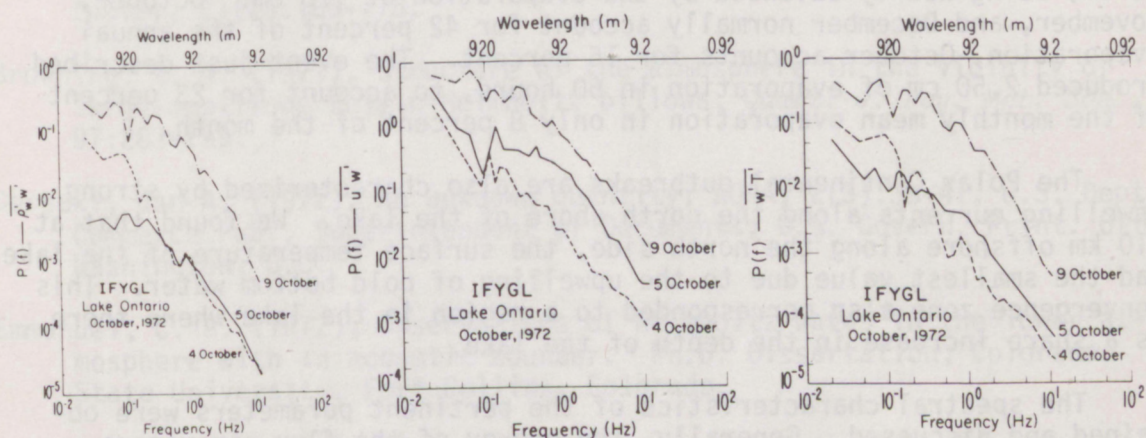


Figure 19. The spectra of water vapor, momentum, and heat obtained on 4, 5, and 9 Oct 1972.

#### 4. CONCLUSIONS

Condensation onto the lake surface appears to be prevalent during the spring. This, of course, is due to the large temperature difference that exists between the surface temperature of the lake and the temperature of the overlying air. For May and June, the surface temperature of the lake was about  $8^\circ\text{C}$  lower than the air temperature at 30 m above the lake surface. August was characterized by near equilibrium temperature distribution between the lake surface and that of the air at 30 m. As a result, both the heat flux and evaporation rate were found to be very small. During October and November, the lake surface temperature was consistently greater than that at 30 m. Both the heat flux and evaporation rate were large and positive.



While the "normal" evaporation rate for October is near  $0.3 \text{ cm day}^{-1}$ , this rate almost quadruples during Polar Continental outbreaks. These are characterized by cold dry air moving down from Canada and accompanied by sustained high winds. On October 9 the winds were  $12 \text{ m s}^{-1}$  over the entire lake. The resultant evaporation rate, at the 30 m level in  $\text{cm day}^{-1}$ , was 0.48 at the north side of the lake, 0.92 at the center, and 1.36 at the south side of the lake. The heat flux also increases from north to south at the 30 m level with the most dramatic increase being from north to center. While there is upward transfer of momentum at the north and center of the lake, the south side is characterized by downward flow of momentum, again at the 30 m level.

The average annual precipitation falling into Lake Ontario is about 80 cm, being nearly balanced by the evaporation of 70 cm. October, November, and December normally account for 42 percent of the annual evaporation, October accounts for 15 percent. The event just described produced 2.50 cm of evaporation in 60 hours, to account for 23 percent of the monthly mean evaporation in only 8 percent of the month.

The Polar Continental outbreaks are also characterized by strong upwelling currents along the north shore of the lake. We found that at 10 km offshore along the north side, the surface temperature of the lake had the smallest value due to the upwelling of cold bottom water. This convergence zone also corresponded to a region in the lake where there is a sharp increase in the depth of the lake.

The spectral characteristics of the pertinent parameters were obtained and discussed. Generally, the energy of the flux parameters increased from north to south and confirmed the results obtained by Bean et al. (1972) during BOMEX.

Derecki (1972) found that the maximum evaporation of  $11.4 \text{ cm}$  (or  $0.38 \text{ cm day}^{-1}$ ) is in September. For October, the evaporation rate is nearly  $0.35 \text{ cm day}^{-1}$ . All these are from surface measurements throughout the lake. We have found that at the 30 m level throughout the lake the evaporation rate is  $0.32 \text{ cm day}^{-1}$  for October.



## 5. REFERENCES

- Bean, B. R., and E. J. Dutton (1966), *Radio Meteorology*, Dover Publications, Inc., New York.
- Bean, B. R., R. E. McGavin, C. B. Emmanuel, and R. W. Krinks (1969), Radio-physical studies of evaporation at Lake Hefner, 1966 and 1967, ESSA Tech. Report, ERL 115-WPL 7, June.
- Bean, B. R., R. Gilmer, R. Grossman, R. McGavin, and C. Travis (1972), An analysis of airborne measurements of vertical water vapor flux during BOMEX, *J. Atmos. Sci.*, 29:860-869.
- Birnbaum, G. A. (1950), Recording microwave refractometer, *Rev. Sci. Instr.*, 21(2):169-176.
- Browning, K. A. (1971), Structure of the atmosphere in the vicinity of large-amplitude Kelvin-Helmholtz billows, *Quart. J. Roy. Met. Soc.*, 97:283-299.
- Derecki, Jan A. (1972), An unknown quantity, NOAA, 2(3):38-41, U.S. Dept. Commerce Pub., Superintendent of Documents, U.S. Govern. Print. Off., Washington, D.C.
- Emmanuel, C. B. (1972), Observations of Helmholtz waves in the lower atmosphere with an acoustic sounder. Ph.D. Dissertation, Colorado State University, Fort Collins, Colorado.
- Emmanuel, C. B. (1973), Richardson number profiles through shear instability wave regions observed in the lower planetary boundary layer, *Boundary Layer Meteorology* 5(1/2):19-27.
- Frenkiel, J. (1963), On the accuracy of the combined energy-budget and mass-transfer method, *J. Geophys. Res.*, 68(17):4989-4992.
- Grossman, R. L., and B. R. Bean (1973), An aircraft investigation of turbulence in the lower layers of a marine boundary layer, NOAA Tech. Rept., ERL 291-WMPO 4, October.
- McBean, G. A., and R. D. Paterson (1974), Variations of the turbulent fluxes of momentum, heat and moisture over Lake Ontario. Submitted for publication in the *J. Phys. Oceanography*.
- McGavin, R. E., and M. J. Vetter (1965), Radio refractometry and its potential for humidity studies, Proc. Intern. Conf. on Humidity and Moisture, II, 553-560 (Reinhold, New York, N.Y.).
- Swinbank, W.C. (1951), The measurement of vertical transfer of heat and water vapor and momentum in the lower atmosphere with some results, *J. Meteorol.*, 8:135-145.



Swinbank, W. C. (1955), An experimental study of eddy transports in the lower atmosphere, *Meteorol. Phys. Tech. Paper No. 2*, Commonwealth Scientific and Industrial Research Organization.

Webb, E. K. (1960), An investigation of the evaporation from Lake Encumbere, *Meteorol. Phys. Tech. Paper No. 10*, Commonwealth Scientific and Industrial Research Organization.

Woods, J. D. (1969), On Richardson's number as a criterion for laminar-turbulent-laminar transition in the ocean and atmosphere, *Radio Science* 4(12):1289-1298.



## APPENDIX A

### GUST PROBE DATA PROCESSING

The parameters measured onboard the RFF DC-6 aircraft are listed below.

$F_{\alpha}$	Force on vertical vane
$F_{\beta}$	Force on horizontal vane
$a_N$	Vertical acceleration (boom)
$a_L$	Lateral acceleration (boom)
$\Delta P$	Pitot pressure
$P$	Pressure
$N$	Refractivity
$T$	Temperature
$\phi$	Roll
$\theta$	Pitch
$a_Z$	Vertical acceleration (c.g.)
$a_F$	Longitudinal acceleration (c.g.)
$\dot{\psi}$	Yaw Rate
$\dot{\phi}$	Roll rate
$\dot{\theta}$	Pitch rate

From these measurements the eddy fluxes of heat, moisture, and momentum are computed. The parameters are measured in analog form, converted to digital and recorded on magnetic tape. The sampling rate is 100 samples per second per channel. Five variables are produced: the three components of the wind,  $u$ ,  $v$ , and  $w$ ; the water vapor density  $\rho_w$ ; and the temperature  $T$ . Means, variances, time series and spectra of each variable and each flux quantity are then obtained.

#### A-1. Basic Measurements

The winds are measured with both a gust probe on the nose boom and an inertial navigational system (INS). The gust probe consists of two fixed vanes, one horizontal and one vertical, arranged around a central pitot tube. The vanes measure the motion of the air relative to the aircraft, accelerometers measure the motion of the boom, and the INS at the center of gravity measures the motion of the aircraft relative to an earth oriented coordinate system.



The water vapor density is determined from the measurement of radio refractive index, which is a function of temperature, pressure, and water vapor density.

The temperature is measured with a small bead thermistor.

Additional parameters can be measured:

Hdg	Heading
DA	Draft angle
$V_X$	Ground speed east
$V_Y$	Ground speed north
$a_S$	Lateral acceleration at center of gravity
$V_T$	True air speed

## A-2. Wind Velocities

The gust probe yields estimates of the fluctuations of the wind relative to the aircraft axis. The aircraft axes can be referred to earth axes by one of two means:

1. Integration of various gravity activated accelerometers to produce the velocity of the aircraft relative to the earth.
2. Use the velocities and heading from the Navigational System.

Hence, a redundancy is possible to check one approach against the other.

In both approaches there are two expressions that must be solved. These are the vertical angle of attack and the lateral angle of attack of the two gust probe vanes.

For the alpha vane, the vertical angle of attack is

$$\Delta\alpha = 2 \frac{\Delta F_{\alpha} + m \Delta a_N}{C_{\alpha} \rho V_T^2 S}$$

where the  $\Delta$ 's indicate detrended data and



$F_{\alpha}$  is in grams = 19.20963391

$a_N$  is in  $m s^{-2}$

$\rho$  is in  $g m^{-3}$

$C_{\alpha}$  is in  $rad^{-1} = 2.755 rad^{-1}$

$V_T$  is in  $m s^{-1}$

$S$  is in  $m^2 = 5.17 \times 10^{-3} m^2$ .

Then

$$\rho = 348.38 \frac{P}{T_V},$$

and

$$V_T^2 = (20.046)^2 EMS \cdot T_V,$$

where  $P$  is in mb

$T_V$  is in  $^{\circ}K$

$EMS$  is the (Mach number) $^2$ .

Thus,

$$\rho V_T = (20.046)^2 EMS \cdot T_V \left( 348.38 \frac{P}{T_V} \right),$$

and

$$\Delta\alpha = 9.829587 \times 10^{-3} \left[ \frac{\Delta F_{\alpha} + 1.960167 \Delta\alpha_N}{P \cdot EMS} \right].$$

Also,  $\Delta\beta$  is computed in identical fashion with  $\alpha$  and  $a_N$  replaced by  $\beta$  and  $a_L$ , respectively.

N.B.  $\Delta\alpha$  is in radians

$F$  is in grams

$a_N$  is in  $m s^{-1}$

$P$  is in mb

$EMS$  is the (Mach number) $^2$ ,

$$EMS = \left[ 5 \left( \frac{P_P}{P_S} + 1 \right)^{2/7} - 1 \right],$$

where  $P_P$  = differential pitot pressure (mb),

$P_S$  = static pressure (mb).



If EMS is expanded in a MacLaurin Series

$$\text{EMS} = 1.4286 \left( \frac{P_P}{P_S} \right) - 0.5102 \left( \frac{P_P}{P_S} \right)^2 + 0.275 \left( \frac{P_P}{P_S} \right)^3 ,$$

then the vertical gust velocity (integrated from accelerometers) is

$$w' = V_T(\Delta\alpha + \Delta\beta\Delta\phi - \Delta\theta) + \int \alpha a_z dt + L_X \Delta\dot{\theta} ,$$

where the angles  $\alpha$ ,  $\beta$ ,  $\phi$ ,  $\theta$  are in radians and

$a_z$  is in  $\text{m s}^{-1}$ ,

$V_T$  is in  $\text{m s}^{-1}$ ,

$w$  is in  $\text{m s}^{-1}$ ,

$L_X$  is in the distance in meters from the gust probe to the location of the measurement of  $\theta$ .

The angles  $\phi$  and  $\theta$  can come either from the roll and pitch gyros or from the INS. The integration of  $a_z$  is done by use of Simpson's Rule, i.e.,

$$\int_{t_n}^{t_n+2\Delta t} X(t) dt = \frac{\Delta t}{3} [X(t_n) + 4X(t_n + \Delta t) + X(t_n + 2\Delta t)] .$$

The cross axis gust component of the wind can be expressed as

$$V' = V_T(\Delta\beta - \Delta\alpha\Delta\phi + \Delta\psi) + \int (\Delta a_L + \Delta a_N \Delta\phi) dt + L_X \Delta\dot{\psi} , \quad (2)$$

where the yaw ( $\psi$ ) came either from the yaw rate gyros or from the oscillations of the heading as measured by the INS. The longitudinal gust component of the wind is expressed as

$$u' = \Delta V_T - \int (\Delta a_F - \Delta a_N \Delta\theta) dt. \quad (3)$$

These are the three gust velocities used to compute the fluxes.



### A-3. Computation of Water Vapor Density and Temperature

It remains now to compute

$\rho_w'$  - the fluctuations of the water vapor density.

$T'$  - the fluctuations of the temperature.

The temperature,  $T$ , is measured using a thermistor that exhibits dynamic heating at aircraft velocities. Hence,

$$T_a = T_i(1 - 0.15 \text{ EMS})$$

where  $T_a$  = ambient temperature in  $^{\circ}\text{K}$ , and  
 $T_i$  = indicate temperature in  $^{\circ}\text{K}$ .

Also the virtual temperature,  $T_v$ , is given by

$$T_v = T_a / (1 - 0.001745 \frac{\rho_v T_a}{P_s}) .$$

The water vapor density,  $\rho_w$ , is measured from the refractometer (N), the temperature ( $T_a$ ), and the pressure ( $P_s$ ), hence

$$\rho_w = 0.0005805(N T_a - 77.6 P_s) .$$

$T_a$  and  $\rho_w$  are then detrended with zero mean values.

### A-4. Computation of Fluxes

The products  $u'w'$ ,  $v'w'$ ,  $T'w'$ , and  $\rho_w'w'$  are then computed. From these data we can get

1. Time series of each variable
2. Time series of the fluxes
3. Means of each variable
4. Means of each flux
5. Variance of each variable
6. Variance of each flux.

Using the Fast Fourier Transform (FFT) subroutine we can get

1. Power spectra of each product
2. Power spectra of each variable.

Although it is not being done, we can get cospectra and quadspectra of the variable in each product.



#### A-5. Error Analysis of the Fluxes

Each of the variables in the above expressions contains error of measurement. Hence, the "answers" contain some uncertainty, i.e., there is an error band on the "answer." If we say one variable is a function of a set of other variables, i.e.,

$$f(a) = f(x, y, z)$$

then

$$dF(a) = \frac{\partial f(a)}{\partial x} dx + \frac{\partial f(a)}{\partial y} dy + \frac{\partial f(a)}{\partial z} dz .$$

The partial derivatives can be determined from average conditions. The derivatives reflect the individual error in the parameters involved. In this case since the means are removed, the error is not based on absolute accuracy but rather in the resolution of each sensor (see main body of this report).

#### A-6. Conversions

Should we wish to convert water vapor flux from units of  $\text{g m}^{-2}\text{s}^{-1}$ , then

1.  $1 \text{ g m}^{-2} \text{ s}^{-1} = 8.64 \text{ cm day}^{-1}$
2. or in terms of latent heat flux  
 $1 \text{ g m}^{-2} \text{ s}^{-1} = 10^{-4} \text{ g cm}^{-2} \text{ s}^{-1}$

Each gram of water that evaporates absorbs the heat of vaporization which is a function of temperature. Running a regression line from  $0^\circ\text{C}$  to  $35^\circ\text{C}$  results in

$$\text{LH (calories)} = -0.563976 T_a + 597.3208/\text{g} .$$

Then, the latent flux  $\text{HF}_L$  is

$$\text{HF}_L = E -0.563976 T_a + 597.3208/\text{g cal m}^{-2} \text{ s}^{-1}$$

$$1 \text{ cal s}^{-1} = 4.18684 \text{ Watts} .$$

$$\text{HF}_L = E [10^{-1} \cdot 4.18684 (-0.563976 T_a + 597.3208)] \text{mW cm}^{-2}$$

$$\text{HF}_L = E [-0.2361277 T_a + 250.0887] \text{mW cm}^{-2} .$$

If the temperature is expressed in  $^\circ\text{K}$

$$\text{HF}_L = E [-0.2361277 T_K + 314.5893] \text{mW cm}^{-2} .$$



If  $\rho$  is assumed to be  $1.2 \times 10^3 \text{ g m}^{-3}$ , then

$$HF_L = 28.9 [E(\text{cm day}^{-1})] \text{mW cm}^{-2} \text{ at } 20^\circ\text{C}.$$

Should we wish to convert  $\overline{T'w'}$  in  $^\circ\text{K m s}^{-1}$  to sensible heat flux  $HF_s$  in  $\text{mW cm}^{-2}$ , then

$$HF_s = \rho C_p \overline{T'w'},$$

where

$$\rho = 348.38 \frac{P}{T_v}$$

$$C_p = 0.240 \text{ cal g}^{-1}\text{K}^{-1}$$

$$HF_s = 348.38 (0.24) \frac{P}{T_v} \overline{T'w'} \text{ mW cal m}^{-2}\text{s}^{-1},$$

$$HF_s = \frac{348.38 (0.24)(4.1855)}{10} \frac{P}{T_v} \overline{T'w'} \text{ mW cm}^{-2}.$$

If  $\rho$  is again assumed to be  $1.2 \times 10^3 \text{ g m}^{-3}$

$$HF_s = 120.6 \overline{T'w'} \text{ mW cm}^{-2} \text{ at } 20^\circ\text{C}.$$

The momentum flux,  $\overline{u'w'}$ , in  $\text{m}^2 \text{s}^{-2}$  can be converted to momentum flux (MF) in  $\text{dynes cm}^{-2}$ . We find

$$MF = 3.4838 \frac{P}{T_v} \overline{u'w'} \text{ dynes cm}^{-2}.$$

Again, if we take  $\rho = 1.2 \times 10^3 \text{ g m}^{-3}$  at  $20^\circ\text{C}$ , then

$$MF = 12 \overline{u'w'} \text{ dynes cm}^{-2}.$$

#### A-7. Calibration

Now it is necessary to consider calibration of each sensor. In most cases, we assume a linear relationship between the actual parameter and the recorder input. (The departure from linearity is accounted for in the error analysis.) For example:



1. Each parameter has a range of values, which is represented by a  $\pm 2.5$  V range in output.
2. The A/D converts  $\pm 2.5$  V to  $\pm 2045$  digital counts.

Then,

$$y = mx + b,$$

where  $y$  is the parameter in engineering units and  $x$  is the digital count.

*Vanes.* A 300 gm weight is used to calibrate the vanes. The vanes are turned in orientation from vertical to horizontal both positive and negative. The output with no weight and then with weights is recorded. From these measurements calibration curves are plotted.

*Accelerometers.* Since these accelerometers are of the shuttle type, changing their orientation relative to earth's gravity (at sea level) provides measurements which are used for calibration.

*Pressure.* A calibrated pressure system is used to calibrate both pitot and static probes.

*Refractivity.* Since refractivity is measured over a restricted scale, two calibrations are required. The average value or center scale, and the slope or gain for departures from the center value. The former is determined by the Assman reading on preflight and postflight. The latter is determined from laboratory calibration. Likewise, the range switching is determined by laboratory calibration.

*Temperature.* Calibrated for center value via the Assman. Gain (slope) and range switching is a laboratory calibration.

*Outputs from INS.* Pitch, roll, heading, and accelerations are calibrated by physically moving the INS (after alignment) over the three axes using a precision level for determining platform attitude.



An example of the calibrations is given below (IFYGL).

x is in digital counts

Parameter	Symbol	Calibration	Units
Roll Angle	$\phi$	$y = 4.469 \cdot 10^{-5}x - 8.165 \cdot 10^{-5}$	rad
Pitch Angle	$\theta$	$y = 4.346 \cdot 10^{-5}x - 1.169 \cdot 10^{-3}$	rad
Roll Rate	$\dot{\phi}$	$y = 1.725 \cdot 10^{-4}x - 0.1772$	rad s <sup>-1</sup>
Yaw Rate	$\dot{\psi}$	$y = 1.696 \cdot 10^{-4}x - 0.1740$	rad s <sup>-1</sup>
Vertical Acceleration (Boom)	$a_N$	$y = 9.631 \cdot 10^{-3}x + 0.0353$	m <sup>-2</sup>
Latitudinal Acceleration (Boom)	$a_L$	$y = 9.580 \cdot 10^{-3}x + 6.386 \cdot 10^{-3}$	m <sup>-2</sup>
Vertical Acceleration (c.g.)	$a_Z$	$y = 2.391 \cdot 10^{-3}x + 0.0263$	m <sup>-2</sup>
Longitudinal Acceleration (c.g.)	$a_F$	$y = 4.787 \cdot 10^{-3}x$	m <sup>-2</sup>
Pressure	P	$y = -0.134709 x + 784.98$	mb
Temperature	T	$y = 2.443 \cdot 10^{-3}x$	°K
Refractivity	N	$y = -7.328 \cdot 10^{-3}x$	N units
Pitot	$\Delta P$	$y = 2.777 \cdot 10^{-2}x + 19.792$	mb
Pitch Rate	$\dot{\theta}$	$y = 1.707 \cdot 10^{-3}x + 0.1626$	rad s <sup>-2</sup>
Alpha Force	$F_{N\alpha}$	$y = 0.1534 x + 13.804$	g
Beta Force	$F_{N\beta}$	$y = 0.1578 x$	g



## APPENDIX B

The time segments shown in table B-1 were fully analyzed and have been submitted to the IFYCL archives. For further analysis as well as for archive storage, the processed data were presented in three basic forms:

1. power spectra on micro-film,
2. time series records on micro-film, and
3. means, variances, fluxes in print-out form.

A time series plot presents a smoothed time series of  $w'$ ,  $v'$ ,  $u'$ ,  $\rho'_w$ , and  $T'$ . All five variables are plotted simultaneously in the time domain at a sample rate of 6.25 samples per second. The means, variances, fluxes, correlation coefficients as well as the Monin-Obukhov stability parameters are computed for 3 minutes or less and use the 50 sample per second data. The spectra programs produce both the time series spectra and the flux or covariance spectra. For ease in the interpretation of the data, the spectra are presented in the following form: (a) log-log (512 spectral estimates plotted), (b) log-log smoothed (28 averaged spectral estimates with even distribution across the frequency range), (c)  $fP(f)$  spectra (512 points), and (d)  $fP(f)$  smoothed spectra (28 points). As an example of this type of presentation we have chosen a time period from the October 9 data. Each shows the variable (U, V, W represent  $u'$ ,  $v'$ ,  $w'$ , respectively), the day, starting and ending time: 283150611 represents the day (283 is 9 October), the hour (15), minutes (06), and seconds (11) after the hour. The following 21 figures are the smoothed spectra of the pertinent parameters as they appear on microfilm submitted to the IFYGL archives.



Table B-1. Analyzed Time Periods from the IFYGL Measurements

START TIME	SAMPLE LENGTH	TOTAL RECORDS	PACKED RECORDS	ALTITUDE	TERRAIN	RELATIVE WIND
127145531	2 MINUTES 59.20 SECONDS	175	35	1000	WATER	DOWNWIND
127150231	2 MINUTES 59.20 SECONDS	175	35	500	WATER	UPWIND
127151031	2 MINUTES 59.20 SECONDS	175	35	100	WATER	DOWNWIND
127152401	2 MINUTES 59.20 SECONDS	175	35	1000	WATER	CROSSWIND
127153000	2 MINUTES 59.20 SECONDS	175	35	500	WATER	CROSSWIND
127153701	2 MINUTES 59.20 SECONDS	175	35	100	WATER	CROSSWIND
127154431	2 MINUTES 59.20 SECONDS	175	35	500	WATER	CROSSWIND
127155701	2 MINUTES 59.20 SECONDS	175	35	1000	WATER	CROSSWIND
127161330	2 MINUTES 59.20 SECONDS	175	35	1000	WATER	CROSSWIND
127161731	2 MINUTES 59.20 SECONDS	175	35	1000	LAND	CROSSWIND
127162131	2 MINUTES 59.20 SECONDS	175	35	1000	LAND	UPWIND
127162531	2 MINUTES 59.20 SECONDS	175	35	1000	LAND	CROSSWIND
130160916	2 MINUTES 43.84 SECONDS	160	32	1000	WATER	CROSSWIND
130161601	2 MINUTES 59.20 SECONDS	175	35	500	WATER	CROSSWIND
130162201	2 MINUTES 59.20 SECONDS	175	35	300	WATER	CROSSWIND
130163100	2 MINUTES 59.20 SECONDS	175	35	100	WATER	CROSSWIND
130164000	2 MINUTES 59.20 SECONDS	175	35	500	WATER	UPWIND
130164451	2 MINUTES 59.20 SECONDS	175	35	100	WATER	UPWIND
130164951	2 MINUTES 38.72 SECONDS	155	31	500	WATER	UPWIND
130165401	2 MINUTES 59.20 SECONDS	175	35	100	WATER	UPWIND
130170001	2 MINUTES 59.20 SECONDS	175	35	1000	WATER	CROSSWIND
130170901	2 MINUTES 59.20 SECONDS	175	35	500	WATER	CROSSWIND
130171611	2 MINUTES 59.20 SECONDS	175	35	300	WATER	CROSSWIND
130172400	2 MINUTES 59.20 SECONDS	175	35	100	WATER	CROSSWIND
130172950	2 MINUTES 59.20 SECONDS	175	35	500	WATER	UPWIND
130174046	2 MINUTES 59.20 SECONDS	175	35	1000	WATER	CROSSWIND
130174730	2 MINUTES 59.20 SECONDS	175	35	500	WATER	CROSSWIND
130175401	2 MINUTES 59.20 SECONDS	175	35	300	WATER	CROSSWIND
130180401	2 MINUTES 59.20 SECONDS	175	35	100	WATER	CROSSWIND
130181702	5 MINUTES 58.40 SECONDS	350	70	500	WATER	CROSSWIND
130195331	2 MINUTES 59.20 SECONDS	175	35	500	WATER	CROSSWIND
130200141	2 MINUTES 59.20 SECONDS	175	35	300	WATER	CROSSWIND
130200946	2 MINUTES 59.20 SECONDS	175	35	100	WATER	UPWIND
130202210	2 MINUTES 59.20 SECONDS	175	35	500	WATER	CROSSWIND
130202631	2 MINUTES 59.20 SECONDS	175	35	100	WATER	CROSSWIND
130203800	2 MINUTES 59.20 SECONDS	175	35	500	WATER	CROSSWIND
130204516	2 MINUTES 59.20 SECONDS	175	35	100	WATER	CROSSWIND
130210101	2 MINUTES 59.20 SECONDS	175	35	1000	WATER	CROSSWIND
131150240	8 MINUTES 57.60 SECONDS	525	105	500	WATER	DOWNWIND
131151501	2 MINUTES 59.20 SECONDS	175	35	100	WATER	DOWNWIND
131152011	2 MINUTES 59.20 SECONDS	175	35	500	WATER	CROSSWIND
131154400	8 MINUTES 57.60 SECONDS	525	105	500	WATER	UPWIND
131155501	2 MINUTES 59.20 SECONDS	175	35	100	WATER	UPWIND
131160000	2 MINUTES 59.20 SECONDS	175	35	500	WATER	UPWIND
131164701	2 MINUTES 59.20 SECONDS	175	35	1000	WATER	UPWIND
131165201	2 MINUTES 59.20 SECONDS	175	35	500	WATER	DOWNWIND
131165800	2 MINUTES 59.20 SECONDS	175	35	300	WATER	UPWIND
131170350	2 MINUTES 59.20 SECONDS	175	35	100	WATER	DOWNWIND
131171001	5 MINUTES 58.40 SECONDS	350	70	500	WATER	DOWNWIND
131172031	2 MINUTES 59.20 SECONDS	175	35	1000	WATER	UPWIND
131172601	2 MINUTES 59.20 SECONDS	175	35	1000	WATER	CROSSWIND
131173101	2 MINUTES 59.20 SECONDS	175	35	500	WATER	CROSSWIND
131173601	2 MINUTES 59.20 SECONDS	175	35	300	WATER	CROSSWIND
131174141	2 MINUTES 59.20 SECONDS	175	35	100	WATER	CROSSWIND
131174631	2 MINUTES 59.20 SECONDS	175	35	500	WATER	CROSSWIND
131175051	2 MINUTES 59.20 SECONDS	175	35	100	WATER	CROSSWIND
131175441	2 MINUTES 59.20 SECONDS	175	35	300	WATER	CROSSWIND
131180231	2 MINUTES 59.20 SECONDS	175	35	1000	WATER	CROSSWIND
131180801	2 MINUTES 59.20 SECONDS	175	35	500	WATER	CROSSWIND
131181321	2 MINUTES 59.20 SECONDS	175	35	300	WATER	CROSSWIND
131182001	2 MINUTES 59.20 SECONDS	175	35	100	WATER	CROSSWIND
131191400	17 MINUTES 55.20 SECONDS	1050	210	300	WATER	UPWIND
131195301	8 MINUTES 57.60 SECONDS	525	105	300	WATER	UPWIND
131151231	2 MINUTES 8.00 SECONDS	125	25	100	WATER	CROSSWIND
131155201	1 MINUTES 27.04 SECONDS	85	17	100	WATER	CROSSWIND
131160730	2 MINUTES 59.20 SECONDS	175	35	1000	WATER	CROSSWIND
131161320	2 MINUTES 59.20 SECONDS	175	35	500	WATER	CROSSWIND
132161930	2 MINUTES 59.20 SECONDS	175	35	300	WATER	CROSSWIND
132162601	2 MINUTES 59.20 SECONDS	175	35	100	WATER	CROSSWIND
132163131	2 MINUTES 59.20 SECONDS	175	35	500	WATER	DOWNWIND
132163601	2 MINUTES 59.20 SECONDS	175	35	100	WATER	CROSSWIND

1 INFORMATION FILE AND 71 DATA FILES ON THIS TAPE











START TIME	SAMPLE LENGTH		TOTAL RECORDS
134162453	5 MINUTES	58.40 SECONDS	350
134163432	2 MINUTES	43.84 SECONDS	160
134164341	5 MINUTES	53.40 SECONDS	350
134165722	2 MINUTES	54.08 SECONDS	170
134170431	2 MINUTES	59.20 SECONDS	175
134171111	2 MINUTES	59.20 SECONDS	175
134173840	2 MINUTES	3.00 SECONDS	125
134175120	2 MINUTES	38.72 SECONDS	155
134180750	2 MINUTES	28.48 SECONDS	145
164173601	2 MINUTES	59.20 SECONDS	175
164175002	2 MINUTES	59.20 SECONDS	175
164180126	8 MINUTES	57.60 SECONDS	525
164181802	2 MINUTES	59.20 SECONDS	175
164182947	8 MINUTES	57.60 SECONDS	525
164184631	2 MINUTES	59.20 SECONDS	175
164185401	8 MINUTES	57.60 SECONDS	525
164190631	2 MINUTES	59.20 SECONDS	175
164191431	2 MINUTES	59.20 SECONDS	175
164193524	2 MINUTES	59.20 SECONDS	175
164194428	8 MINUTES	57.60 SECONDS	525
164195832	2 MINUTES	59.20 SECONDS	175
167170750	2 MINUTES	59.20 SECONDS	175
167171241	2 MINUTES	59.20 SECONDS	175
167171811	2 MINUTES	38.72 SECONDS	155
167172332	1 MINUTES	47.52 SECONDS	105
167183711	2 MINUTES	18.24 SECONDS	135
167184131	2 MINUTES	59.20 SECONDS	175
167184841	2 MINUTES	59.20 SECONDS	175
167185618	2 MINUTES	59.20 SECONDS	175
167190311	2 MINUTES	59.20 SECONDS	175
167190831	2 MINUTES	59.20 SECONDS	175
168143200	1 MINUTES	57.76 SECONDS	115
168144111	2 MINUTES	28.48 SECONDS	145
168145052	2 MINUTES	59.20 SECONDS	175
168150431	2 MINUTES	59.20 SECONDS	175
168151434	8 MINUTES	57.60 SECONDS	525
168153007	2 MINUTES	59.20 SECONDS	175
168154023	11 MINUTES	56.80 SECONDS	700
168155706	2 MINUTES	59.20 SECONDS	175
168160713	8 MINUTES	57.60 SECONDS	525
168162156	2 MINUTES	59.20 SECONDS	175
168163635	11 MINUTES	56.80 SECONDS	700
168165450	2 MINUTES	59.20 SECONDS	175
168170412	8 MINUTES	57.60 SECONDS	525
168171939	2 MINUTES	59.20 SECONDS	175
168173041	2 MINUTES	59.20 SECONDS	175
168175557	8 MINUTES	57.60 SECONDS	525
168182031	2 MINUTES	59.20 SECONDS	175
168183743	2 MINUTES	59.20 SECONDS	175
168184732	8 MINUTES	57.60 SECONDS	525

PACKED RECORDS	ALTITUDE	TERRAIN	RELATIVE WIND
70	500	WATER	DOWNWIND
32	100	WATER	
70	1000	WATER	
34	1000	LAND	
35	300	WATER	
35	100	WATER	UPWIND
25	60	WATER	
31	60	WATER	
29	60	WATER	
35	100	WATER	CROSWIND
35	100	WATER	DOWNWIND
105	100	WATER	DOWNWIND
35	100	WATER	CROSWIND
105	100	WATER	UPWIND
35	500	WATER	
105	500	WATER	
35	500	WATER	
35	500	WATER	UPWIND
35	1000	WATER	CROSWIND
105	1000	WATER	DOWNWIND
35	1000	WATER	CROSWIND
35	500	WATER	DOWNWIND
35	300	WATER	UPWIND
31	100	WATER	DOWNWIND
21	60	WATER	UPWIND
27	300	WATER	DOWNWIND
35	100	WATER	UPWIND
35	60	WATER	DOWNWIND
35	500	WATER	CROSWIND
35	300	WATER	DOWNWIND
35	100	WATER	UPWIND
23	60	WATER	UPWIND
29	60	WATER	UPWIND
35	60	WATER	DOWNWIND
35	100	WATER	CROSWIND
105	100	WATER	DOWNWIND
35	100	WATER	CROSWIND
140	100	WATER	UPWIND
35	500	WATER	CROSWIND
105	500	WATER	DOWNWIND
35	500	WATER	CROSWIND
140	500	WATER	UPWIND
35	1000	WATER	UPWIND
105	1000	WATER	CROSWIND
35	1000	WATER	CROSWIND
35	1000	WATER	UPWIND
105	1000	LAND	
35	60	WATER	UPWIND
35	100	WATER	CROSWIND
105	100	WATER	DOWNWIND



START TIME	SAMPLE LENGTH		TOTAL RECORDS	PACKED RECORDS	ALTITUDE	TERRAIN	RELATIVE WIND
168190209	2 MINUTES	53.20 SECONDS	175	35	100	WATER	CROSSWIND
168191257	11 MINUTES	56.60 SECONDS	700	140	100	WATER	UPWIND
168192926	2 MINUTES	59.20 SECONDS	175	35	500	WATER	CROSSWIND
168193822	8 MINUTES	57.60 SECONDS	525	105	500	WATER	DOWNWIND
168195240	2 MINUTES	53.20 SECONDS	175	35	500	WATER	CROSSWIND
1 INFORMATION FILE AND		55 DATA FILES ON THIS TAPE					



START TIME	SAMPLE LENGTH		TOTAL RECORDS	PACKED RECORDS	ALTITUDE	TERRAIN	RELATIVE WIND
169151140	2 MINUTES	59.20 SECONDS	175	35	500	WATER	DOWNWIND
169151811	2 MINUTES	59.20 SECONDS	175	35	300	WATER	UPWIND
169152551	2 MINUTES	59.20 SECONDS	175	35	100	WATER	UPWIND
169153401	2 MINUTES	59.20 SECONDS	175	35	60	WATER	DOWNWIND
169155050	2 MINUTES	59.20 SECONDS	175	35	500	WATER	CROSWIND
169155621	2 MINUTES	59.20 SECONDS	175	35	300	WATER	CROSWIND
169160251	2 MINUTES	59.20 SECONDS	175	35	100	WATER	CROSWIND
169160941	2 MINUTES	59.20 SECONDS	175	35	60	WATER	CROSWIND
169162610	2 MINUTES	59.20 SECONDS	175	35	500	WATER	UPWIND
169163231	2 MINUTES	59.20 SECONDS	175	35	300	WATER	DOWNWIND
169164311	2 MINUTES	59.20 SECONDS	175	35	100	WATER	UPWIND
169165151	2 MINUTES	59.20 SECONDS	175	35	60	WATER	CROSWIND
169170801	5 MINUTES	58.40 SECONDS	350	70	500	WATER	CROSWIND
169171651	2 MINUTES	59.20 SECONDS	175	35	500	WATER	CROSWIND
169172241	2 MINUTES	59.20 SECONDS	175	35	300	WATER	CROSWIND
169172901	2 MINUTES	59.20 SECONDS	175	35	100	WATER	CROSWIND
171151351	2 MINUTES	59.20 SECONDS	175	35	500	WATER	DOWNWIND
171151931	2 MINUTES	59.20 SECONDS	175	35	300	WATER	UPWIND
171152552	2 MINUTES	59.20 SECONDS	175	35	1000	WATER	DOWNWIND
171153142	2 MINUTES	59.20 SECONDS	175	35	500	WATER	CROSWIND
171153732	2 MINUTES	59.20 SECONDS	175	35	1000	WATER	CROSWIND
171154420	2 MINUTES	59.20 SECONDS	175	35	500	WATER	CROSWIND
171154942	2 MINUTES	59.20 SECONDS	175	35	500	WATER	CROSWIND
171155411	2 MINUTES	59.20 SECONDS	175	35	500	WATER	UPWIND
171160021	2 MINUTES	59.20 SECONDS	175	35	1000	WATER	DOWNWIND
171164531	2 MINUTES	59.20 SECONDS	175	35	1000	WATER	CROSWIND
171165941	1 MINUTE	59.80 SECONDS	700	140	500	WATER	CROSWIND
171174531	2 MINUTES	59.20 SECONDS	175	35	60	WATER	CROSWIND
172150551	2 MINUTES	59.20 SECONDS	175	35	1000	WATER	DOWNWIND
172151211	2 MINUTES	59.20 SECONDS	175	35	500	WATER	UPWIND
172151841	2 MINUTES	59.20 SECONDS	175	35	300	WATER	DOWNWIND
172152601	2 MINUTES	59.20 SECONDS	175	35	100	WATER	UPWIND
172153351	2 MINUTES	59.20 SECONDS	175	35	60	WATER	DOWNWIND
172153951	2 MINUTES	59.20 SECONDS	175	35	500	WATER	CROSWIND
172154521	2 MINUTES	59.20 SECONDS	175	35	1000	WATER	CROSWIND
172155251	2 MINUTES	59.20 SECONDS	175	35	500	WATER	CROSWIND
172155931	2 MINUTES	59.20 SECONDS	175	35	300	WATER	CROSWIND
172161030	2 MINUTES	59.20 SECONDS	175	35	60	WATER	CROSWIND
172161651	2 MINUTES	59.20 SECONDS	175	35	500	WATER	CROSWIND
172162411	2 MINUTES	59.20 SECONDS	175	35	1000	WATER	CROSWIND
172162951	2 MINUTES	59.20 SECONDS	175	35	500	WATER	CROSWIND
172163621	2 MINUTES	59.20 SECONDS	175	35	300	WATER	CROSWIND
172164341	2 MINUTES	59.20 SECONDS	175	35	60	WATER	CROSWIND
172173121	8 MINUTES	57.60 SECONDS	525	105	500	WATER	UPWIND
172180330	2 MINUTES	59.20 SECONDS	175	35	60	WATER	DOWNWIND
224174430	0 MINUTES	56.32 SECONDS	55	11	500	WATER	CROSWIND
224175110	1 MINUTES	47.52 SECONDS	105	21	500	WATER	CROSWIND
228140330	2 MINUTES	59.20 SECONDS	175	35	1000	WATER	DOWNWIND
228141300	2 MINUTES	59.20 SECONDS	175	35	500	WATER	UPWIND
228142011	2 MINUTES	59.20 SECONDS	175	35	300	WATER	DOWNWIND
228142831	2 MINUTES	59.20 SECONDS	175	35	100	WATER	UPWIND
228143631	2 MINUTES	59.20 SECONDS	175	35	60	WATER	DOWNWIND
228144731	2 MINUTES	59.20 SECONDS	175	35	1500	WATER	UPWIND
228145451	11 MINUTES	56.80 SECONDS	700	140	500	WATER	UPWIND
228152051	2 MINUTES	59.20 SECONDS	175	35	100	WATER	DOWNWIND
228152641	5 MINUTES	58.40 SECONDS	350	70	100	WATER	DOWNWIND
228153931	2 MINUTES	59.20 SECONDS	175	35	1000	LAND	UPWIND
228154345	2 MINUTES	59.20 SECONDS	175	35	1000	WATER	UPWIND
228155135	5 MINUTES	58.40 SECONDS	350	70	1000	WATER	UPWIND
228155946	2 MINUTES	2.88 SECONDS	120	24	1000	LAND	UPWIND
228172351	2 MINUTES	59.20 SECONDS	175	35	1000	WATER	CROSWIND
228173101	2 MINUTES	59.20 SECONDS	175	35	500	WATER	CROSWIND
228173811	2 MINUTES	59.20 SECONDS	175	35	300	WATER	DOWNWIND
228174511	2 MINUTES	59.20 SECONDS	175	35	100	WATER	UPWIND
228175330	2 MINUTES	59.20 SECONDS	175	35	60	WATER	DOWNWIND
228180611	2 MINUTES	59.20 SECONDS	175	35	500	WATER	CROSWIND
228181211	2 MINUTES	59.20 SECONDS	175	35	100	WATER	CROSWIND
229151011	1 MINUTES	21.92 SECONDS	80	16	1000	LAND	
229151336	2 MINUTES	59.20 SECONDS	175	35	1000	WATER	
229152044	2 MINUTES	2.88 SECONDS	120	24	1000	LAND	
229161952	2 MINUTES	59.20 SECONDS	175	35	1000	WATER	
229162701	2 MINUTES	59.20 SECONDS	175	35	500	WATER	
229163441	2 MINUTES	59.20 SECONDS	175	35	300	WATER	
229164251	2 MINUTES	59.20 SECONDS	175	35	100	WATER	CROSWIND
229165501	2 MINUTES	59.20 SECONDS	175	35	1000	WATER	CROSWIND
229170231	2 MINUTES	48.96 SECONDS	165	33	500	WATER	CROSWIND
229170831	1 MINUTES	37.28 SECONDS	95	19	100	WATER	CROSWIND
229171015	2 MINUTES	13.12 SECONDS	130	26	100	WATER	CROSWIND
229171631	2 MINUTES	59.20 SECONDS	175	35	60	WATER	DOWNWIND

1 INFORMATION FILE AND 79 DATA FILES ON THIS TAPE



START TIME	SAMPLE LENGTH	TOTAL RECORDS
160200621	11 MINUTES 56.80 SECONDS	700
160202453	2 MINUTES 59.20 SECONDS	175
160203510	8 MINUTES 57.60 SECONDS	525
160204931	2 MINUTES 59.20 SECONDS	175
160210005	8 MINUTES 57.60 SECONDS	525
160212516	8 MINUTES 57.60 SECONDS	525
270145301	2 MINUTES 59.20 SECONDS	175
270150002	2 MINUTES 59.20 SECONDS	175
270151411	2 MINUTES 59.20 SECONDS	175
270152130	2 MINUTES 59.20 SECONDS	175
270152732	2 MINUTES 59.20 SECONDS	175
270153331	2 MINUTES 59.20 SECONDS	175
270153911	2 MINUTES 59.20 SECONDS	175
270154501	2 MINUTES 59.20 SECONDS	175
270155110	2 MINUTES 59.20 SECONDS	175
270155631	2 MINUTES 59.20 SECONDS	175
270161731	2 MINUTES 59.20 SECONDS	175
270162450	2 MINUTES 59.20 SECONDS	175
270163931	2 MINUTES 59.20 SECONDS	175
270164711	2 MINUTES 59.20 SECONDS	175
270165331	2 MINUTES 59.20 SECONDS	175
270170411	5 MINUTES 58.40 SECONDS	350
270171940	2 MINUTES 59.20 SECONDS	175
270172745	5 MINUTES 58.40 SECONDS	350
270174510	2 MINUTES 59.20 SECONDS	175
270150121	2 MINUTES 59.20 SECONDS	175
270150841	2 MINUTES 59.20 SECONDS	175
270151541	2 MINUTES 59.20 SECONDS	175
270152401	2 MINUTES 59.20 SECONDS	175
270153211	2 MINUTES 59.20 SECONDS	175
270154110	6 MINUTES 57.60 SECONDS	525
270164041	2 MINUTES 59.20 SECONDS	175
270164730	2 MINUTES 59.20 SECONDS	175
270165411	2 MINUTES 59.20 SECONDS	175
270170150	2 MINUTES 59.20 SECONDS	175
270171004	6 MINUTES 57.60 SECONDS	525
270172420	8 MINUTES 57.60 SECONDS	525
270174250	8 MINUTES 57.60 SECONDS	525
270180231	2 MINUTES 59.20 SECONDS	175
270180711	2 MINUTES 59.20 SECONDS	175
270181211	2 MINUTES 59.20 SECONDS	175
270181821	2 MINUTES 59.20 SECONDS	175
270182421	2 MINUTES 59.20 SECONDS	175

1 INFORMATION FILE AND 43 DATA FILES ON THIS TAPE

PACKED RECORDS	ALTITUDE	WATER	RELATIVE WIND
140	500	WATER	UPWIND
35	1000	WATER	CROSSWIND
105	1000	WATER	DOWNWIND
35	1000	WATER	CROSSWIND
105	1000	WATER	UPWIND
105	1000	LAND	CROSSWIND
35	1000	WATER	CROSSWIND
35	500	WATER	CROSSWIND
35	60	WATER	CROSSWIND
35	100	WATER	CROSSWIND
35	500	WATER	DOWNWIND
35	500	WATER	CROSSWIND
35	300	WATER	CROSSWIND
35	100	WATER	DOWNWIND
35	60	WATER	CROSSWIND
35	1000	WATER	CROSSWIND
35	500	WATER	CROSSWIND
35	500	WATER	CROSSWIND
35	100	WATER	UPWIND
35	60	WATER	DOWNWIND
35	1000	WATER	UPWIND
70	300	WATER	CROSSWIND
35	100	WATER	CROSSWIND
70	1000	WATER	CROSSWIND
35	500	WATER	UPWIND
35	1000	WATER	CROSSWIND
35	500	WATER	CROSSWIND
35	300	WATER	CROSSWIND
35	100	WATER	CROSSWIND
35	60	WATER	CROSSWIND
105	1000	WATER	DOWNWIND
35	500	WATER	CROSSWIND
35	300	WATER	CROSSWIND
35	100	WATER	CROSSWIND
35	60	WATER	CROSSWIND
105	500	WATER	UPWIND
105	100	WATER	DOWNWIND
105	100	WATER	UPWIND
35	1000	WATER	CROSSWIND
35	500	WATER	CROSSWIND
35	100	WATER	CROSSWIND
35	60	WATER	CROSSWIND
35	100	WATER	CROSSWIND



START TIME	SAMPLE LENGTH	TOTAL RECORDS	PACKED RECORDS	ALTITUDE	TERRAIN	RELATIVE WIND
203130901	2 MINUTES 59.20 SECONDS	175	35	1000	WATER	QTRWIND
203131701	2 MINUTES 59.20 SECONDS	175	35	500	WATER	QTRWIND
203132431	2 MINUTES 59.20 SECONDS	175	35	300	WATER	QTRWIND
203133421	2 MINUTES 59.20 SECONDS	175	35	100	WATER	CROSWIND
203134351	0 MINUTES 57.60 SECONDS	525	105	300	WATER	CROSWIND
203143401	2 MINUTES 59.20 SECONDS	175	35	1000	LAND	QTRWIND
203143921	2 MINUTES 59.20 SECONDS	175	35	1000	WATER	CROSWIND
203145131	2 MINUTES 59.20 SECONDS	175	35	500	WATER	CROSWIND
203145031	2 MINUTES 59.20 SECONDS	175	35	300	WATER	CROSWIND
203150611	2 MINUTES 59.20 SECONDS	175	35	100	WATER	CROSWIND
203151431	2 MINUTES 59.20 SECONDS	175	35	300	WATER	DOWNWIND
203152240	2 MINUTES 59.20 SECONDS	175	35	1000	WATER	QTRWIND
203153001	2 MINUTES 59.20 SECONDS	175	35	500	WATER	UPWIND
203153721	2 MINUTES 59.20 SECONDS	175	35	300	WATER	QTRWIND
203154551	2 MINUTES 59.20 SECONDS	175	35	100	WATER	UPWIND
203155251	2 MINUTES 59.20 SECONDS	175	35	300	WATER	QTRWIND
203160551	2 MINUTES 59.20 SECONDS	175	35	1000	WATER	DOWNWIND
203161221	2 MINUTES 59.20 SECONDS	175	35	500	WATER	CROSWIND
203161901	2 MINUTES 59.20 SECONDS	175	35	300	WATER	CROSWIND
203162611	2 MINUTES 59.20 SECONDS	175	35	100	WATER	CROSWIND
203170741	2 MINUTES 59.20 SECONDS	175	35	1000	LAND	CROSWIND
203171235	20 MINUTES 54.40 SECONDS	1225	245	1000	WATER	UPWIND
203173731	11 MINUTES 56.00 SECONDS	700	140	500	WATER	DOWNWIND
203180041	23 MINUTES 53.60 SECONDS	1400	280	300	WATER	UPWIND
204142220	2 MINUTES 59.20 SECONDS	175	35	1000	WATER	QTRWIND
204143101	2 MINUTES 59.20 SECONDS	175	35	100	WATER	QTRWIND
204143831	2 MINUTES 59.20 SECONDS	175	35	300	WATER	QTRWIND
204144711	2 MINUTES 59.20 SECONDS	175	35	60	WATER	QTRWIND
204145531	2 MINUTES 59.20 SECONDS	175	35	500	WATER	UPWIND
204150251	2 MINUTES 59.20 SECONDS	175	35	500	WATER	CROSWIND
204151101	2 MINUTES 59.20 SECONDS	175	35	100	WATER	QTRWIND
204151903	17 MINUTES 55.20 SECONDS	1050	210	300	WATER	QTRWIND
204154150	2 MINUTES 59.20 SECONDS	175	35	1000	LAND	UPWIND
204161718	2 MINUTES 59.20 SECONDS	175	35	100	WATER	QTRWIND
204162421	2 MINUTES 59.20 SECONDS	175	35	300	WATER	QTRWIND
204163121	2 MINUTES 59.20 SECONDS	175	35	60	WATER	QTRWIND
204163740	2 MINUTES 59.20 SECONDS	175	35	500	WATER	QTRWIND
204164451	2 MINUTES 59.20 SECONDS	175	35	1000	WATER	QTRWIND
204165041	2 MINUTES 59.20 SECONDS	175	35	300	WATER	CROSWIND
204165911	2 MINUTES 59.20 SECONDS	175	35	1000	WATER	QTRWIND
204170551	2 MINUTES 59.20 SECONDS	175	35	500	WATER	QTRWIND
204171321	2 MINUTES 59.20 SECONDS	175	35	300	WATER	QTRWIND
204172041	2 MINUTES 59.20 SECONDS	175	35	100	WATER	QTRWIND
204172751	2 MINUTES 59.20 SECONDS	175	35	60	WATER	QTRWIND
204173741	2 MINUTES 59.20 SECONDS	175	35	300	WATER	CROSWIND
204174700	2 MINUTES 59.20 SECONDS	175	35	1000	WATER	QTRWIND
204175251	2 MINUTES 59.20 SECONDS	175	35	500	WATER	QTRWIND
204180011	2 MINUTES 59.20 SECONDS	175	35	100	WATER	QTRWIND
204180720	2 MINUTES 43.84 SECONDS	160	32	60	WATER	QTRWIND
204181432	2 MINUTES 59.20 SECONDS	175	35	300	WATER	QTRWIND



START TIME	SAMPLE LENGTH		TOTAL RECORDS
284184431	2 MINUTES	59.20 SECONDS	175
284184835	11 MINUTES	56.80 SECONDS	700
284190240	8 MINUTES	57.60 SECONDS	525
284193000	2 MINUTES	59.20 SECONDS	175
284194001	2 MINUTES	59.20 SECONDS	175
284194711	2 MINUTES	59.20 SECONDS	175

1 INFORMATION FILE AND 56 DATA FILES ON THIS TAPE

PACKED RECORDS	ALTITUDE	TERRAIN	RELATIVE WIND
35	1000	LAND	QTRWIND
140	1000	WATER	CROS WIND
105	500	WATER	CROS WIND
35	500	WATER	
35	60	WATER	
35	300	WATER	



START TIME	SAMPLE LENGTH		TOTAL RECORDS	PACKED RECORDS	ALTITUDE	TERRAIN	RELATIVE WIND
321153930	2 MINUTES	59.20 SECONDS	175	35	1000	WATER	UPWIND
321154501	2 MINUTES	59.20 SECONDS	175	35	1000	WATER	DOWNWIND
321155201	2 MINUTES	59.20 SECONDS	175	35	500	WATER	CROSSWIND
321155730	2 MINUTES	59.20 SECONDS	175	35	500	WATER	DOWNWIND
321160531	2 MINUTES	59.20 SECONDS	175	35	300	WATER	UPWIND
321161201	2 MINUTES	59.20 SECONDS	175	35	300	WATER	CROSSWIND
321162001	2 MINUTES	59.20 SECONDS	175	35	100	WATER	CROSSWIND
321162731	2 MINUTES	59.20 SECONDS	175	35	100	WATER	CROSSWIND
321163831	11 MINUTES	56.80 SECONDS	700	140	300	WATER	CROSSWIND
321170001	2 MINUTES	59.20 SECONDS	175	35	1000	WATER	UPWIND
321170531	2 MINUTES	59.20 SECONDS	175	35	1000	WATER	CROSSWIND
321171331	2 MINUTES	59.20 SECONDS	175	35	500	WATER	CROSSWIND
321171901	2 MINUTES	59.20 SECONDS	175	35	500	WATER	DOWNWIND
321172500	2 MINUTES	59.20 SECONDS	175	35	300	WATER	UPWIND
321173241	2 MINUTES	59.20 SECONDS	175	35	300	WATER	CROSSWIND
321174530	11 MINUTES	56.80 SECONDS	700	140	300	WATER	CROSSWIND
321180621	2 MINUTES	59.20 SECONDS	175	35	1000	WATER	UPWIND
321181231	2 MINUTES	59.20 SECONDS	175	35	1000	WATER	DOWNWIND
321181830	2 MINUTES	59.20 SECONDS	175	35	500	WATER	UPWIND
321182402	2 MINUTES	59.20 SECONDS	175	35	500	WATER	DOWNWIND
321183141	2 MINUTES	59.20 SECONDS	175	35	300	WATER	CROSSWIND
321183901	2 MINUTES	59.20 SECONDS	175	35	300	WATER	DOWNWIND
323151330	2 MINUTES	59.20 SECONDS	175	35	1000	WATER	CROSSWIND
323152131	2 MINUTES	59.20 SECONDS	175	35	500	WATER	UPWIND
323152831	2 MINUTES	59.20 SECONDS	175	35	500	WATER	CROSSWIND
323153501	2 MINUTES	59.20 SECONDS	175	35	300	WATER	CROSSWIND
323154230	2 MINUTES	59.20 SECONDS	175	35	300	WATER	CROSSWIND
323155131	2 MINUTES	59.20 SECONDS	175	35	100	WATER	UPWIND
323155831	2 MINUTES	59.20 SECONDS	175	35	100	WATER	CROSSWIND
323160801	5 MINUTES	58.40 SECONDS	350	70	300	WATER	DOWNWIND
323161801	17 MINUTES	55.20 SECONDS	1050	210	300	WATER	DOWNWIND
323164601	2 MINUTES	59.20 SECONDS	175	35	1000	WATER	CROSSWIND
323165200	2 MINUTES	59.20 SECONDS	175	35	1000	WATER	DOWNWIND
323165831	2 MINUTES	59.20 SECONDS	175	35	500	WATER	UPWIND
323170401	2 MINUTES	59.20 SECONDS	175	35	500	WATER	CROSSWIND
323171131	2 MINUTES	59.20 SECONDS	175	35	300	WATER	CROSSWIND
323171801	2 MINUTES	59.20 SECONDS	175	35	300	WATER	DOWNWIND
323172831	11 MINUTES	56.80 SECONDS	700	140	500	WATER	UPWIND
323174530	2 MINUTES	59.20 SECONDS	175	35	1000	WATER	UPWIND
324163630	2 MINUTES	59.20 SECONDS	175	35	500	WATER	CROSSWIND
324164301	2 MINUTES	59.20 SECONDS	175	35	500	WATER	CROSSWIND
324164831	2 MINUTES	59.20 SECONDS	175	35	300	WATER	CROSSWIND
324165501	2 MINUTES	59.20 SECONDS	175	35	300	WATER	CROSSWIND
324170201	2 MINUTES	59.20 SECONDS	175	35	100	WATER	CROSSWIND
324170901	2 MINUTES	59.20 SECONDS	175	35	100	WATER	CROSSWIND
324171631	2 MINUTES	59.20 SECONDS	175	35	1000	WATER	CROSSWIND
324172201	2 MINUTES	59.20 SECONDS	175	35	1000	WATER	CROSSWIND
324173101	14 MINUTES	56.00 SECONDS	875	175	500	WATER	CROSSWIND
324175001	2 MINUTES	59.20 SECONDS	175	35	1000	WATER	CROSSWIND
324175730	2 MINUTES	59.20 SECONDS	175	35	300	WATER	CROSSWIND



START TIME	SAMPLE LENGTH		TOTAL RECORDS	PACKED RECORDS	ALTITUDE	TERRAIN	RELATIVE WIND
326152131	2 MINUTES	59.20 SECONDS	175	35	1000	WATER	CROSSWIND
326152801	2 MINUTES	59.20 SECONDS	175	35	500	WATER	CROSSWIND
326154401	2 MINUTES	59.20 SECONDS	175	35	300	WATER	CROSSWIND
326155101	2 MINUTES	59.20 SECONDS	175	35	100	WATER	CROSSWIND
326155741	2 MINUTES	59.20 SECONDS	175	35	100	WATER	UPWIND
326160531	2 MINUTES	59.20 SECONDS	175	35	1000	WATER	CROSSWIND
326161221	2 MINUTES	59.20 SECONDS	175	35	500	WATER	CROSSWIND
326161831	2 MINUTES	59.20 SECONDS	175	35	300	WATER	CROSSWIND
326162551	2 MINUTES	59.20 SECONDS	175	35	100	WATER	CROSSWIND
326163430	2 MINUTES	59.20 SECONDS	175	35	100	WATER	UPWIND
326164301	2 MINUTES	59.20 SECONDS	175	35	500	WATER	UPWIND
326164951	2 MINUTES	59.20 SECONDS	175	35	300	WATER	CROSSWIND
326165801	2 MINUTES	59.20 SECONDS	175	35	100	WATER	CROSSWIND
326170631	2 MINUTES	59.20 SECONDS	175	35	60	WATER	CROSSWIND
326172600	2 MINUTES	59.20 SECONDS	175	35	1000	LAND	CROSSWIND
326175731	8 MINUTES	57.60 SECONDS	525	105	1000	WATER	DOWNWIND

1 INFORMATION FILE AND 66 DATA FILES ON THIS TAPE

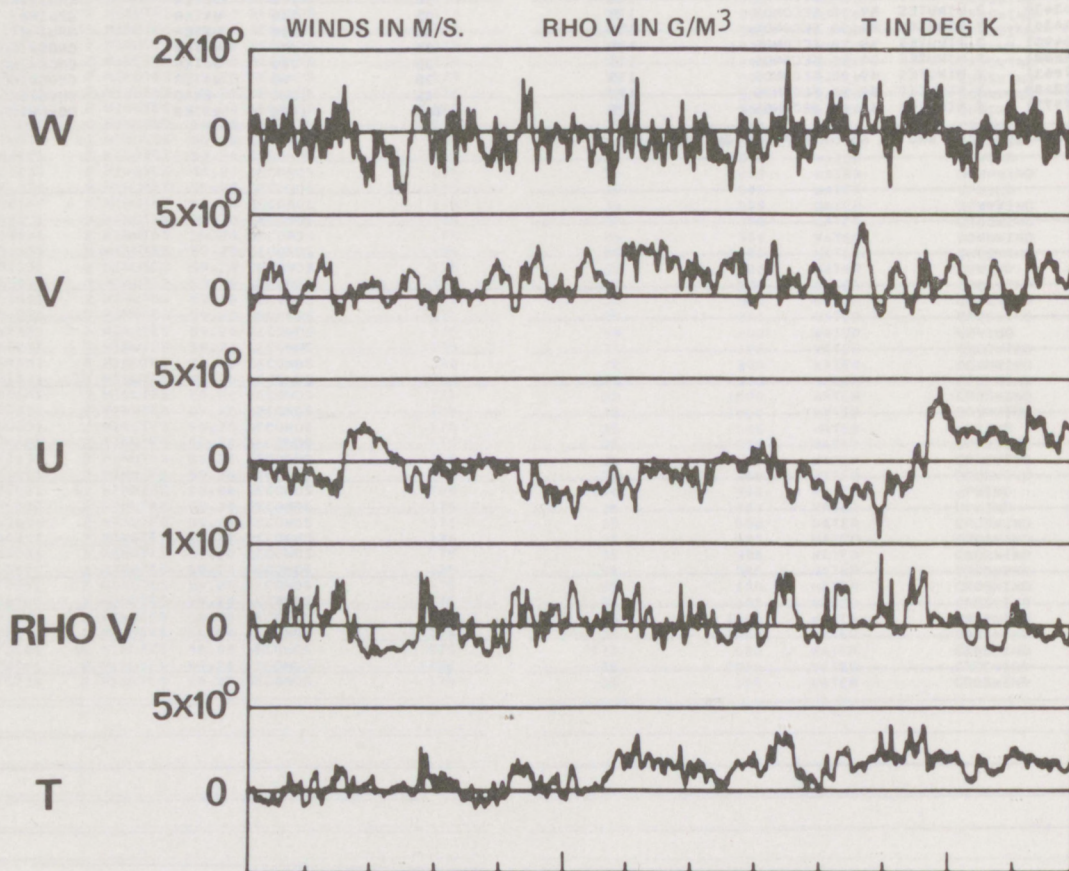


IFYGL

283150611

283150818

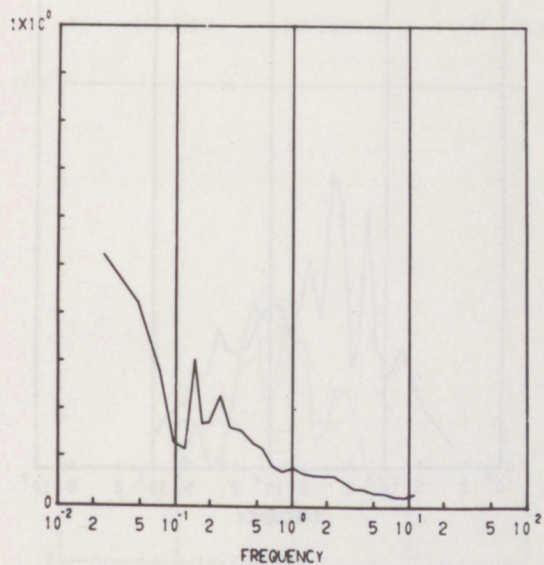
TIME SERIES



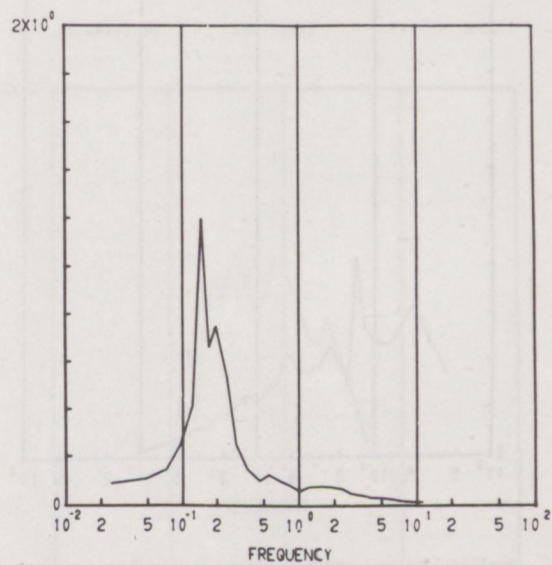
*Time series records of the atmospheric variables as they appear on microfilm submitted to the IFYGL archives.*



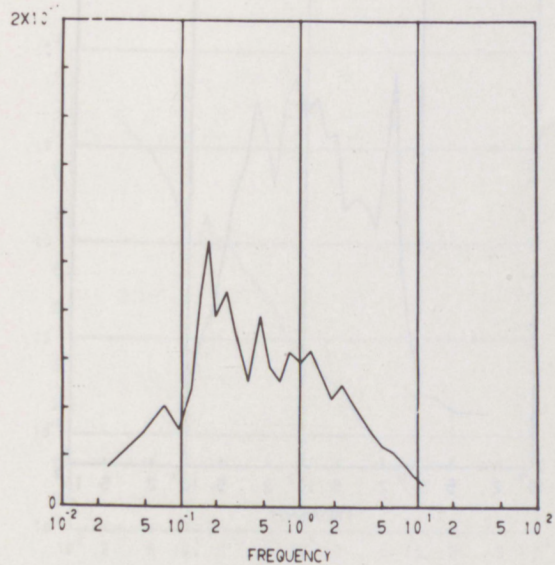
U 283150611 283150909 F1P(F) SMOOTH



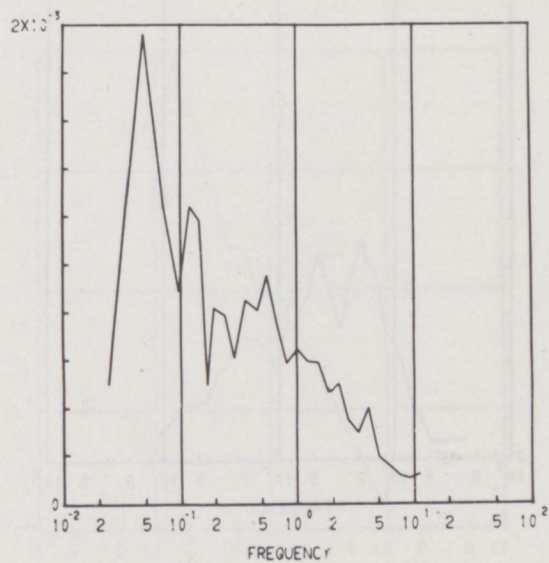
V 283150611 283150909 F1P(F) SMOOTH



X 283151611 283150909 F1P(F) SMOOTH

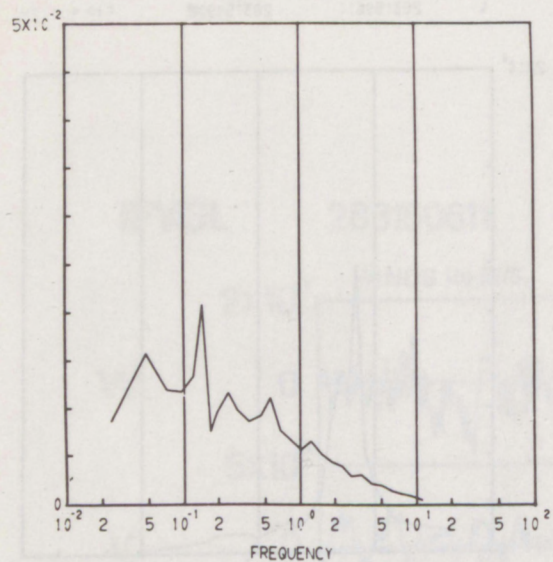


T 283150611 283150909 F1P(F) SMOOTH

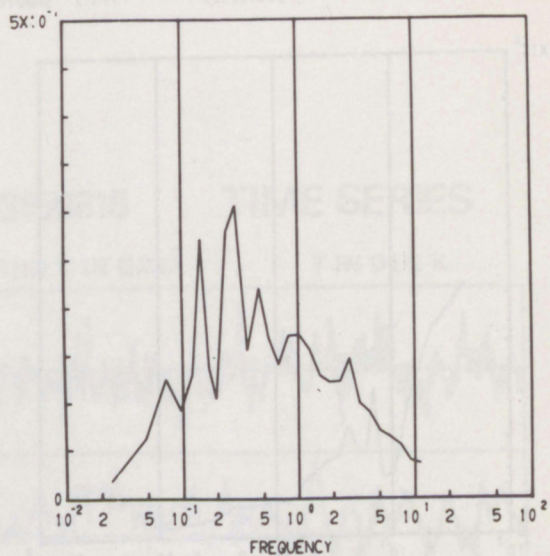




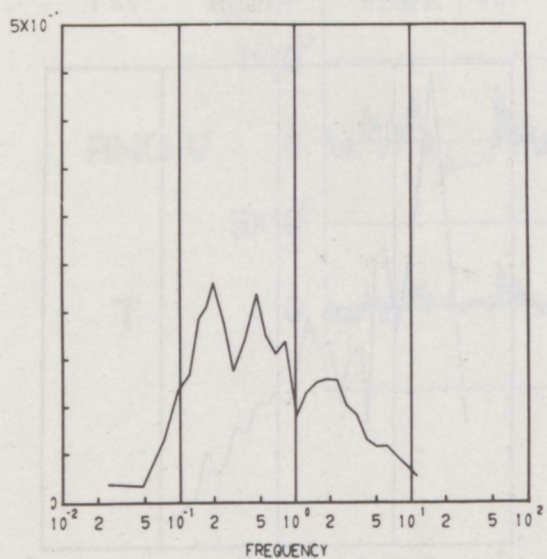
RHO V 283150611 283150909 F&P(F) SMOOTH



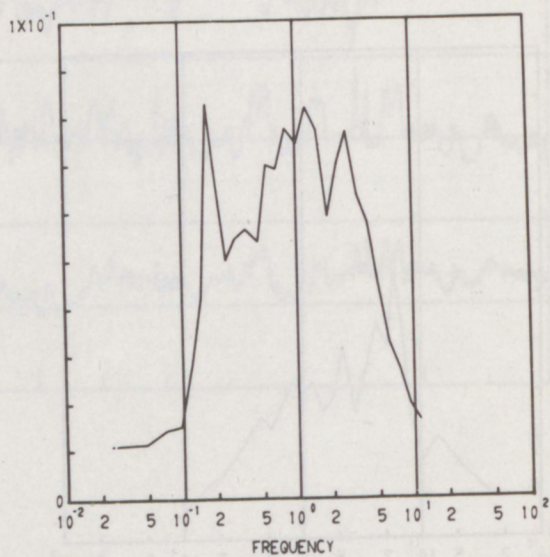
UW 283150611 283150909 F&P(F) SMOOTH



VW 283150611 283150909 F&P(F) SMOOTH

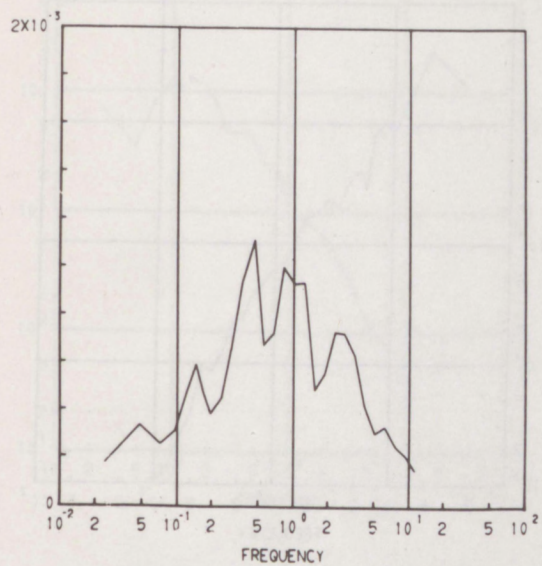


WW 283150611 283150909 F&P(F) SMOOTH

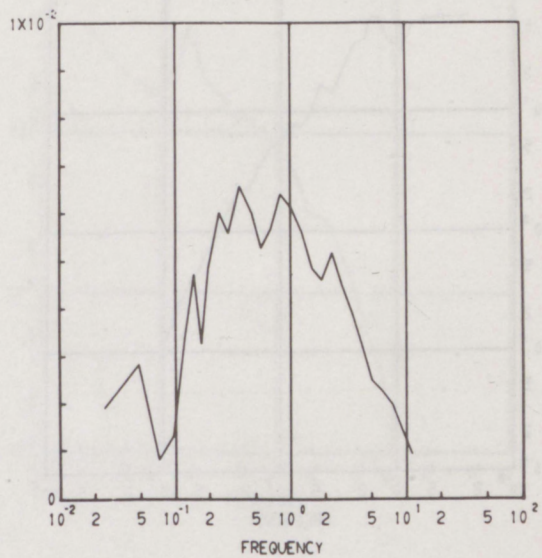




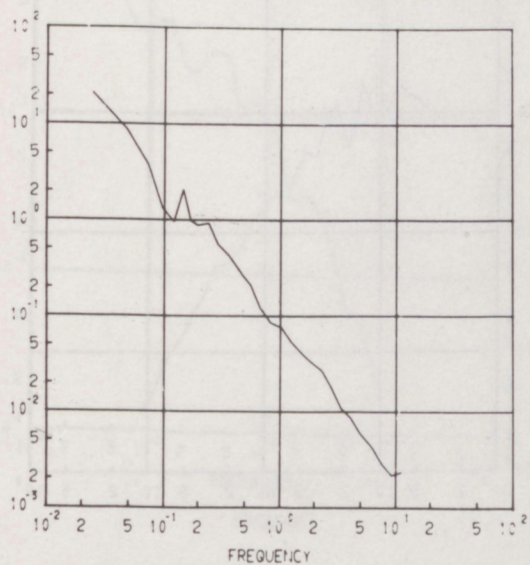
TW 283150611 283150909 F1P1F1 SMOOTH



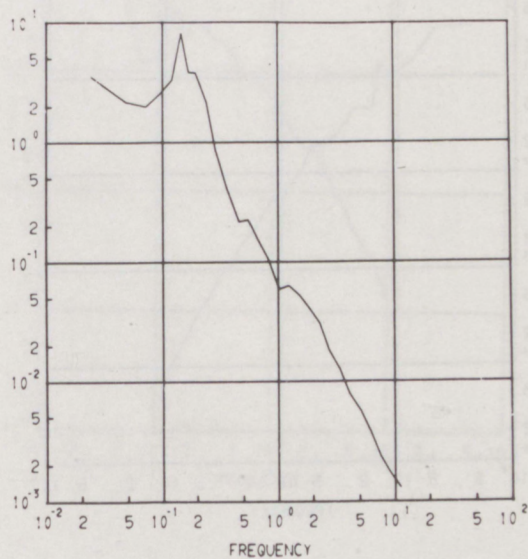
PW 283150611 283150909 F1P1F1 SMOOTH



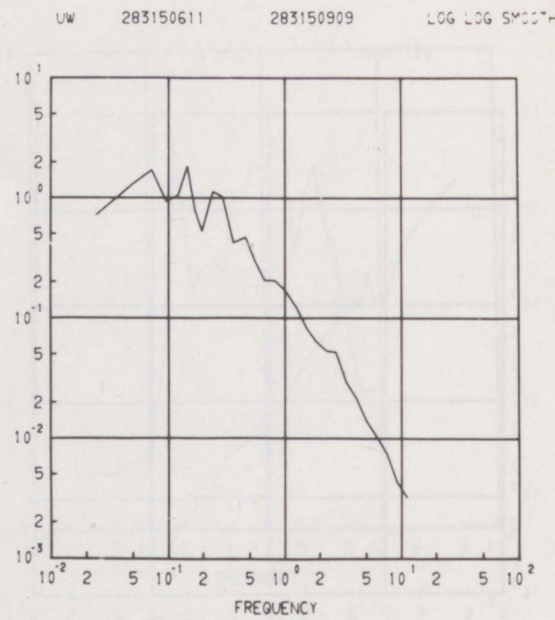
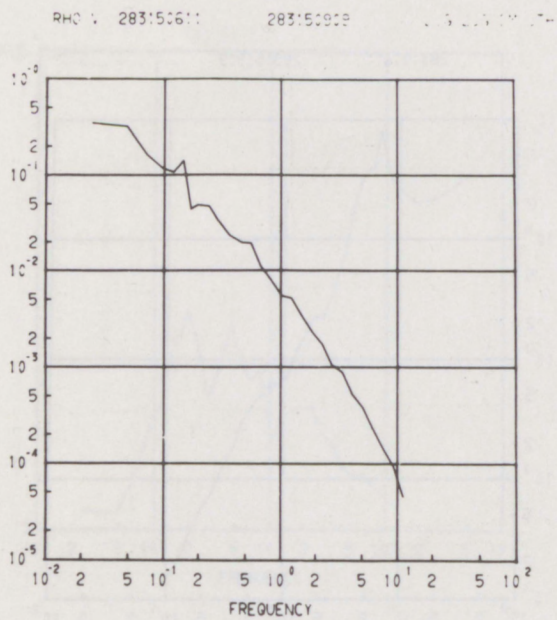
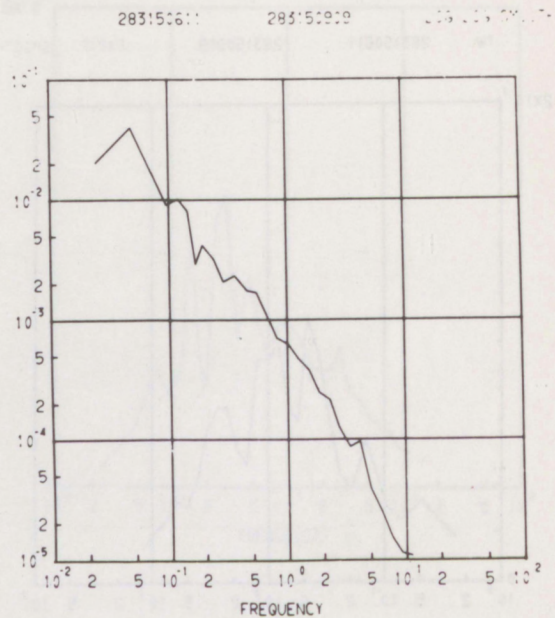
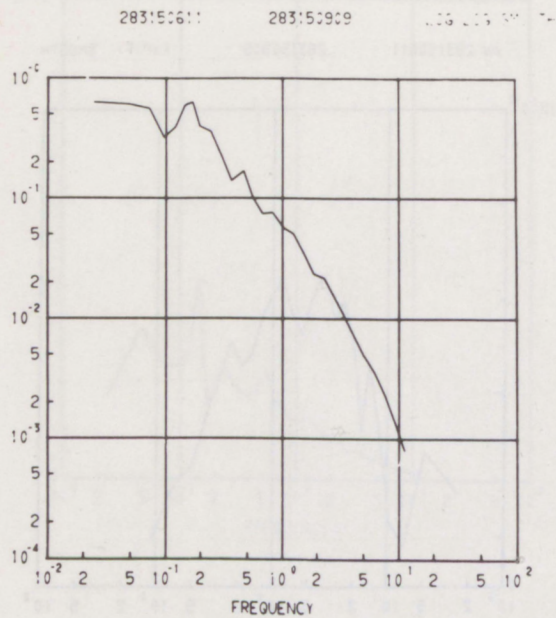
283150611 283150909 LOG LOG SMOOTH



V 283150611 283150909 LOG LOG SMOOTH

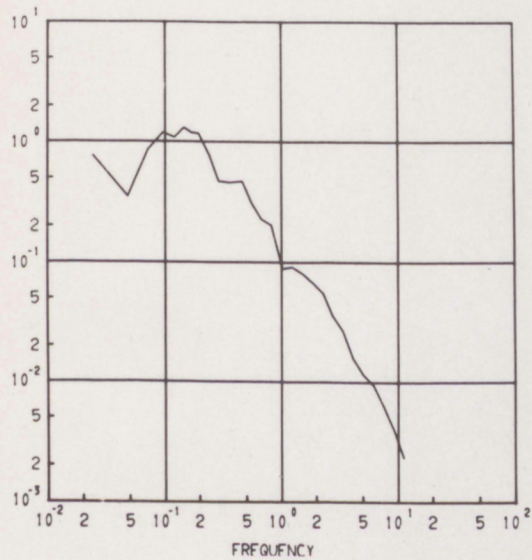




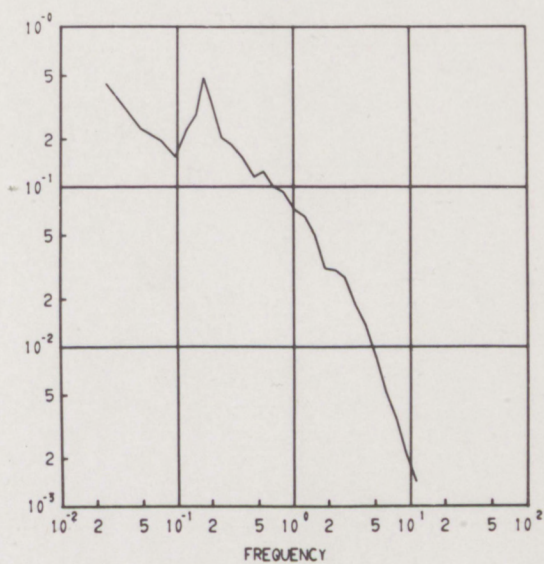




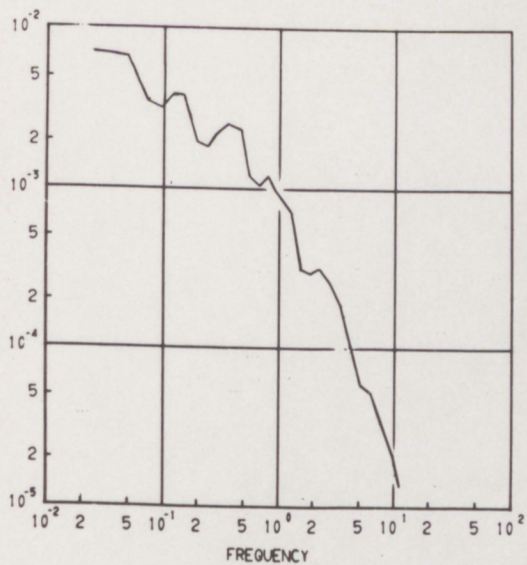
VW 283150611 283150909 LOG LOG SMOOTH



WW 283150611 283150909 LOG LOG SMOOTH



TW 283150611 283150909 LOG LOG SMOOTH



pW 283150611 283150909 LOG LOG SMOOTH

